Supporting Information
for
Cerium(IV) Carboxylate Photocatalyst for Catalytic Radical Formation from Carboxylic Acids: Decarboxylative Oxygenation of Aliphatic Carboxylic Acids and Lactonization of Aromatic Carboxylic Acids

Satoru Shirase,[†] Sota Tamaki,[†] Koichi Shinohara,[†] Keishi Hirosawa,[‡] Hayato Tsurugi,*[1,†]
Tetsuya Satoh,*[2,‡] and Kazushi Mashima*[3,†]
*[1]tsurugi@chem.es.osaka-u.ac.jp, *[2]satoh@sci.osaka-cu.ac.jp, *[3]mashima@chem.es.osaka-u.ac.jp

[†] Department of Chemistry, Graduate School of Engineering Science, Osaka University,
Toyonaka, Osaka 560-8531, Japan.
‡ Department of Chemistry, Graduate School of Science, Osaka City University,
3-3-138 Sugimoto, Sumiyoshi-ku, Osaka 558-8585, Japan

Contents

I. General Procedure

All manipulations involving air- and moisture-sensitive compounds were carried out under an argon atmosphere by using standard vacuum line and Schlenk tube techniques or Ar-filled glovebox. Dry toluene (H_2O, <1 ppm, Kanto Chemical, toluene dehydrated -Super^2 Plus-) was purchased and purified by using Grubbs Column (Glass Counter Solvent Dispending System, Nikko Hansen & Co, Ltd.).[1] Toluene-d_8 and CD_2Cl_2 were purchased and purified by distillation over CaH_2. All other reagents were purchased at the highest commercial quality and used without further purification. $Ce(O^tBu)_4$ was prepared according to the literature.[2] ^{1}H NMR spectral data of all carbonyl compounds **2a-2y**, **3a-3x**, **10** and **12** are superimposed to the corresponding commercially available compounds. NMR yields of products were determined by integral ratios of signals for 1,3,5-trimethoxybenzene (internal standard) and RC*H*O (**2a-2v**), Ar*H* (**2w-2x, 12**), C(C*H*$_3$)$_3$ (**2y**), R*CH*$_2$OH (**3a-3v**), R$_2$C*H*OH (**3w-3x**), or (C*H*$_3$)$_2$ (**10**, **11**) in the ^{1}H NMR spectra. ^{1}H NMR (400 MHz) and ^{13}C{^{1}H} NMR (100 MHz) spectra were measured on Bruker Avance III-400 spectrometers in 5 mm NMR tubes. All ^{1}H NMR chemical shifts were reported in ppm relative to the TMS proton in chloroform-d_1 at δ 0.00. All ^{13}C{^{1}H} NMR chemical shifts were reported in ppm relative to deuterated solvents such as CD_2Cl_2 at δ 53.84, and $CDCl_3$ at δ 77.16. All ^{19}F NMR chemical shifts were reported in ppm. UV-Vis spectra were measured using an Agilent 8453 UV-Vis spectroscopy system. X-ray crystallographic study of **6** was performed on Rigaku XtaLAB P200 system with graphite-monochromated Mo Kα radiation (λ = 0.71075). Melting point of **6** was recorded on BUCHI melting point M-565. ESI-MS spectra were recorded on a Bruker MicroTOF II-HB using Agilent ESI-L Low Concentration Tuning Mix as a reference. Elemental analyses were recorded by using Perkin-Elmer 2400 at the Faculty of Engineering Science, Osaka University.

II. Optimization of Reaction Conditions for Decarboxylative Oxygenation of 1a

All manipulations were conducted under aerobic condition. To a catalyst placed in a test tube (size: φ 15 mm x 130 mm) was added a mixture of carboxylic acid **1a** and internal standard (1,3,5-trimethoxybenzene or α,α,α-trifluoromethylbenzene) in *N,N*-dimethylacetamide (DMA) (0.7 mL). The reaction mixture was irradiated with 40W blue LEDs with stirring at room temperature under air. For determining the yield of the decarboxylative oxygenation products by ^{1}H NMR measurement, a portion of the reaction mixture was diluted with $CDCl_3$, and signal intensities due to the aldehyde hydrogen of **2a** and methylene hydrogens of **3a** and **4a** were calculated with respect to the internal standard.

Table S1. Catalyst Screening in *N,N*-Dimethylacetamide (DMA)[a]

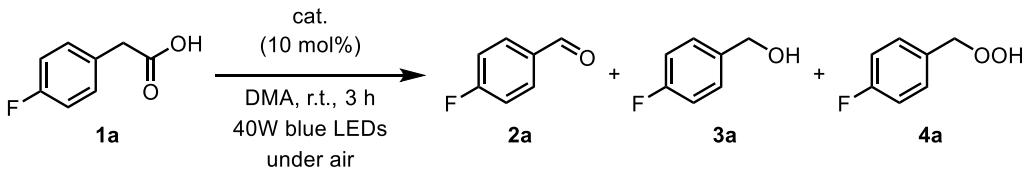

entry	cat.	NMR yields (%)		
		2a	**3a**	**4a**
1	$Ce(O^tBu)_4$	61	<5	20
2	$Ce(OH)_4$	11	n.d.	18
3	$[NH_4][Ce(NO_3)_6]$	n.d.	n.d.	n.d.
4	$Ce(OAc)_3{\cdot}H_2O$	10	n.d.	41
5	$CeCl_3{\cdot}7H_2O$	n.d.	n.d.	n.d.
6	$Ce(NO_3)_3{\cdot}6H_2O$	n.d.	n.d.	n.d.
7	$Ce(acac)_3{\cdot}H_2O$	n.d.	n.d.	<5
8	$Cu(OAc)_2{\cdot}H_2O$	n.d.	n.d.	n.d.
9	$Mn(OAc)_3{\cdot}2H_2O$	n.d.	n.d.	n.d.
10	$Mn(OAc)_2{\cdot}4H_2O$	n.d.	n.d.	n.d.
11	$Mn(acac)_2{\cdot}2H_2O$	n.d.	n.d.	<5
12	$Fe(OAc)_2$	19	n.d.	n.d.
13	$Fe(OH)(OAc)_2$	69	<5	n.d.
14	$Fe(acac)_3$	<5	n.d.	<5
15	$Co(OAc)_2{\cdot}4H_2O$	n.d.	n.d.	n.d.
16	$Co(acac)_2{\cdot}2H_2O$	n.d.	n.d.	n.d.
17	AgOAc	6	<5	n.d.

18	$Ti(O^tBu)_4$	n.d.	n.d.	n.d.
19	$Hf(O^nBu)_4$	n.d.	n.d.	n.d.
20	CeO_2 powder (Aldrich: <25 nm)	n.d.	n.d.	<5
21	CeO_2 powder (Aldrich: <50 nm)	n.d.	n.d.	<5

[a] Reaction conditions: **1a** (0.065 mmol), $Ce(O^tBu)_4$ (10 mol%), DMA (0.7 mL), under air, 40W blue LEDs, 1,3,5-trimethoxybenzene or α,α,α-trifluoromethylbenzene as an internal standard.

Table S2. Solvent Screening[a]

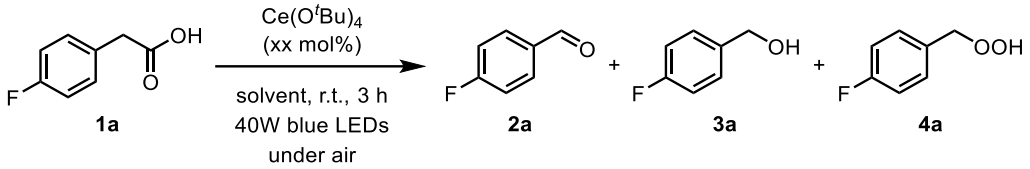

entry	xx mol%	solvent	NMR yields (%)		
			2a	**3a**	**4a**
1	10	DMA	61	<5	20
2	10	*N*,*N*-dimethylformamide	45	n.d.	26
3	10	dimethylsulfoxide	<5	n.d.	30
4	10	*N*-methylpyrrolidone	12	n.d.	34
5	10	mesitylene	80	20	trace
6	10	toluene	85	15	trace
7	5	toluene	86	14	n.d.
8	5	CH_3CN	73	12	7
9	5	dichloroethane	6	<5	61
10	5	DMA	7	n.d.	28
11	5	THF	8	7	32
12	5	EtOH	6	<5	24
13	5	toluene[b]	13	5	59
14	5	toluene[b] with 10 mol% of H_2O	28	11	61
15	5	toluene[b] with 100 mol% of H_2O	79	21	n.d.

[a] Reaction conditions: **1a** (0.100 mmol), $Ce(O^tBu)_4$ (5 or 10 mol%), solvent (1.5 mL), under air, 40W blue LEDs, 1,3,5-trimethoxybenzene as an internal standard. [b] Commercially available dry toluene (H_2O, <1 ppm, Kanto Chemical, toluene dehydrated -Super[2] Plus-) was further purified by passing through Grubbs Column system.

Table S3. Cerium Catalyst Screening in toluene or CH_3CN[a]

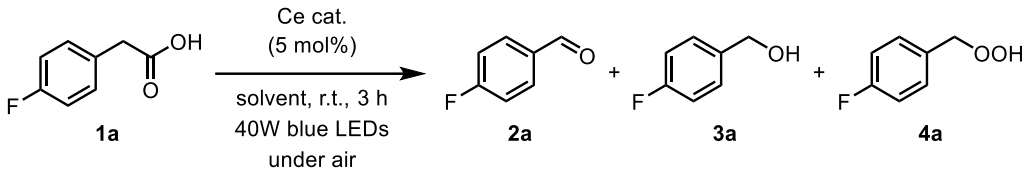

entry	Ce cat.	solvent	NMR yields (%)		
			2a	**3a**	**4a**
1	$Ce(O^tBu)_4$	toluene	86	14	n.d.
2	$Ce(OH)_4$	toluene	n.d.	n.d.	7
3	$[NH_4][Ce(NO_3)_6]$	toluene	n.d.	n.d.	n.d.
4	$Ce(OAc)_3·H_2O$	toluene	n.d.	n.d.	7
5	$CeCl_3·7H_2O$	toluene	n.d.	n.d.	n.d.
6	$Fe(OAc)_2$	toluene	<5	n.d.	n.d.
7	$Fe(OH)(OAc)_2$	toluene	16	9	n.d.
8	$Ce(O^tBu)_4$	CH_3CN	72	12	7
9	$Ce(OH)_4$	CH_3CN	n.d.	n.d.	6
10	$[NH_4][Ce(NO_3)_6]$	CH_3CN	n.d.	n.d.	n.d.
11	$Ce(OAc)_3·H_2O$	CH_3CN	n.d.	n.d.	<5
12	$CeCl_3·7H_2O$	CH_3CN	n.d.	n.d.	n.d.
13	$CeCl_3·7H_2O$ / 25 mol% of $^nBu_4NCl$	CH_3CN	44	20	19
14	$CeCl_3·7H_2O$ / 10 mol% of Cs_2CO_3	CH_3CN	n.d.	n.d.	64

[a] Reaction conditions: **1a** (0.100 mmol), Ce cat. (5 mol%), solvent (1.5 mL), under air, 40W blue LEDs, 1,3,5-trimethoxybenzene as an internal standard.

III. Decarboxylative Oxygenation of 1a by 6 under the Optimized Reaction Conditions

To a yellow powder of **6** (2.3 mg, 5 mol% on Ce with respect to **1a**) in a test tube was added a mixture of **1a** (0.100 mmol) and 1,3,5-trimethoxybenzene in toluene (1.5 mL). The mixture was irradiated by blue LEDs at room temperature for 6 h to give 83% yield of **2a** and 17% yield of **3a** along with the formation of trace amounts of pivalaldehyde and neopentyl alcohol derived from neopentyl carboxylate ligands of **6** (Figure S1).

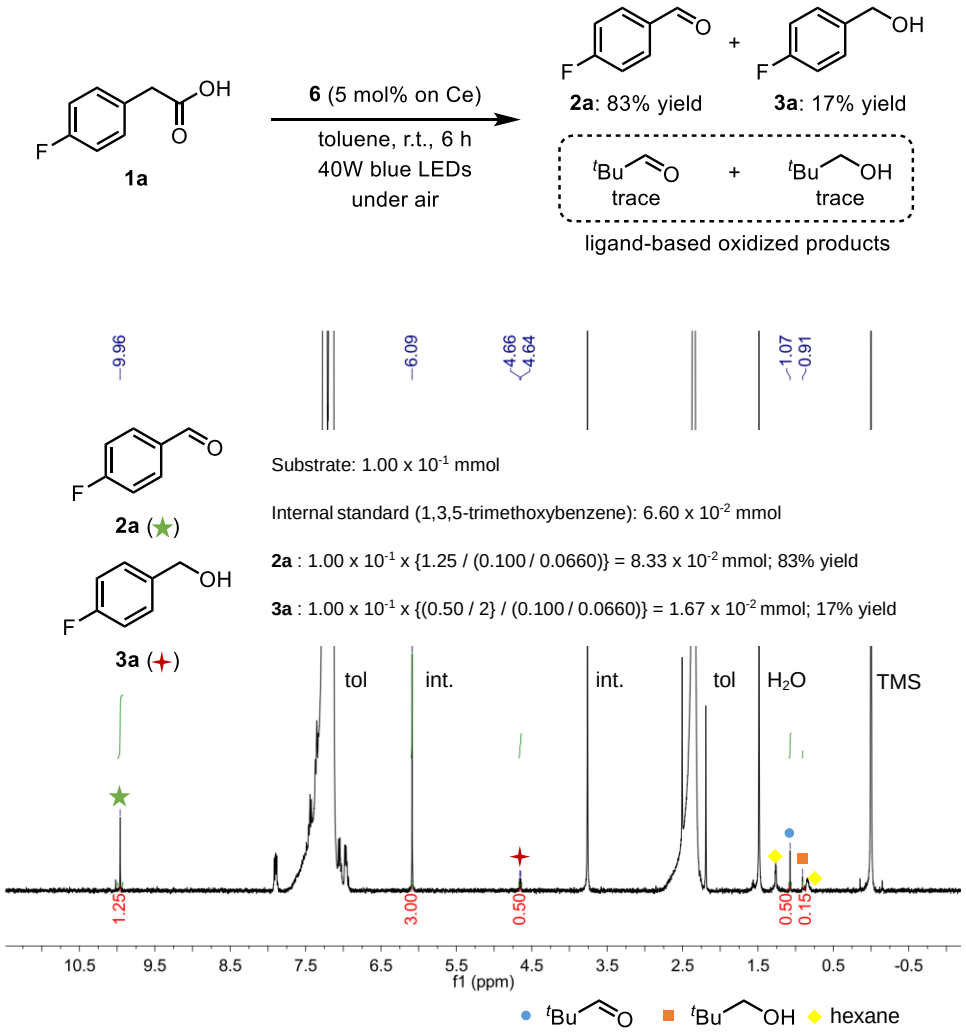

Figure S1. ^{1}H NMR spectrum of the catalytic reaction mixture using **6** as a catalyst.

IV. ESI-MS and UV-Vis Spectra of the Mixture of $Ce(O^tBu)_4$ and 1a in Toluene

A colorless solution of **1a** (0.100 mmol) in 1.5 mL of toluene was added to yellow powder of $Ce(O^tBu)_4$ (0.0050 mmol) at room temperature to give yellow solution. We detected hexanuclear cerium(IV) cluster-derived signals assignable as $\{[\mathbf{5}]_2\text{-}2H^+\}^{2-}$ (**5** = $Ce_6O_4(OH)_4(OCOCH_2C_6H_4F)_{12}$) in the ESI-MS spectrum (eq S1, Figure S2). UV-Vis spectra of the mixture of $Ce(O^tBu)_4$ (6.7 mM) with 10 equiv of **1a** in toluene showed broad absorption below 500 nm (Figure S3).

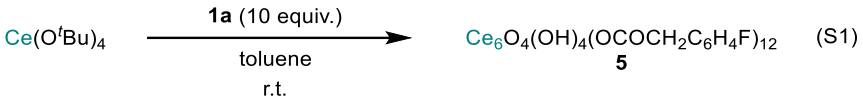

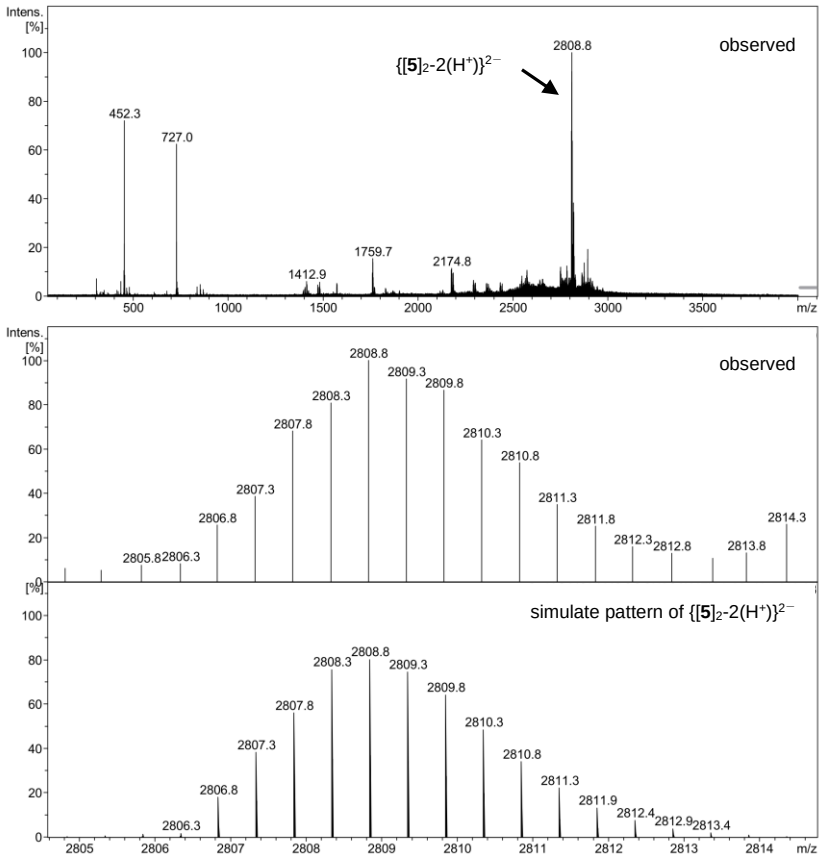

Figure S2. ESI-MS spectra of the mixture of $Ce(O^tBu)_4$ and 10 equiv of **1a** in toluene at negative mode.

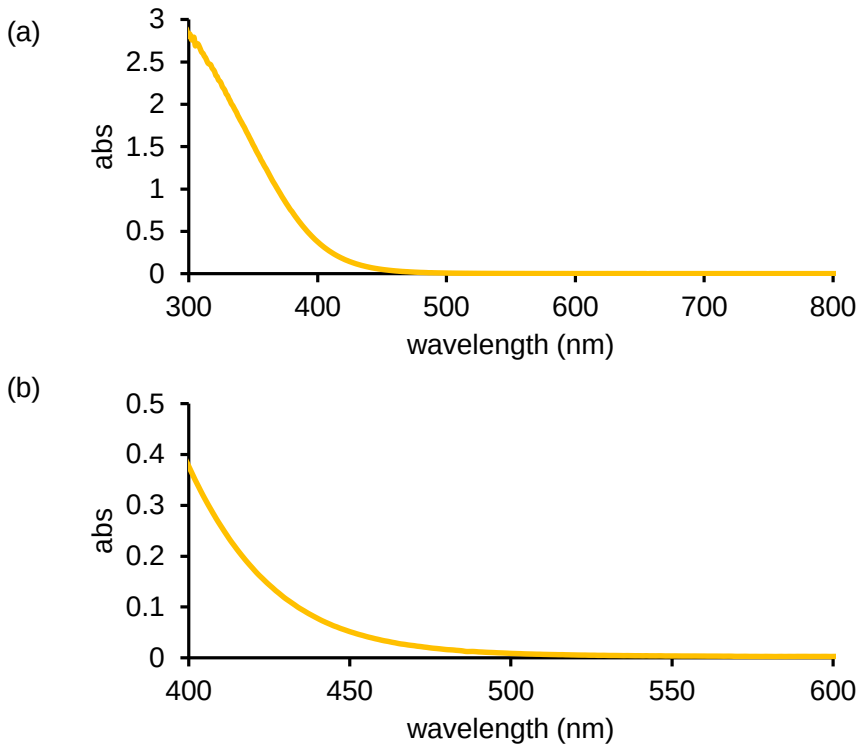

Figure S3. UV-Vis spectra of a reaction mixture of $Ce(O^tBu)_4$ (6.7 mM) with **1a** (10 equiv) in toluene: (a) 300-800 nm, (b) 400-600 nm.

V. Reaction of Ce(O^{t}Bu)$_4$ and 1a in Anhydrous Toluene

Following reaction was conducted under argon atmosphere. To a yellow powder of Ce(O^{t}Bu)$_4$ (43.3 mg, 0.100 mmol) in a screw vial was added a colorless solution of **1a** (61.6 mg, 0.400 mmol) in 1.5 mL of anhydrous toluene[a] at room temperature. A resulting orange suspension was stirred at room temperature for 1 h (eq S2). The supernatant was removed by decantation and the precipitates was washed with anhydrous toluene (0.5 mL x 4) to give 48.0 mg of Ce(OCOCH$_2$C$_6$H$_4$F)$_4$ (63% yield) as an orange powder. ^{1}H NMR (400 MHz, THF-d_8, 303 K): δ 3.10-4.00 (br, 8 H), 6.60-7.70 (br, 16 H). ^{19}F NMR (376 MHz, THF-d_8, 303K): δ 117.6 (s). Anal. calcd for Ce(OCOCH$_2$C$_6$H$_4$F)$_4$: Ce-C$_{32}$H$_{24}$O$_8$F$_4$: C, 51.07; H, 3.21. Found C, 50.98; H, 3.22.

[a] Commercially available dry toluene (H$_2$O, <1 ppm, Kanto Chemical, toluene dehydrated -Super^2 Plus-) was further dried by Grubbs Column system.

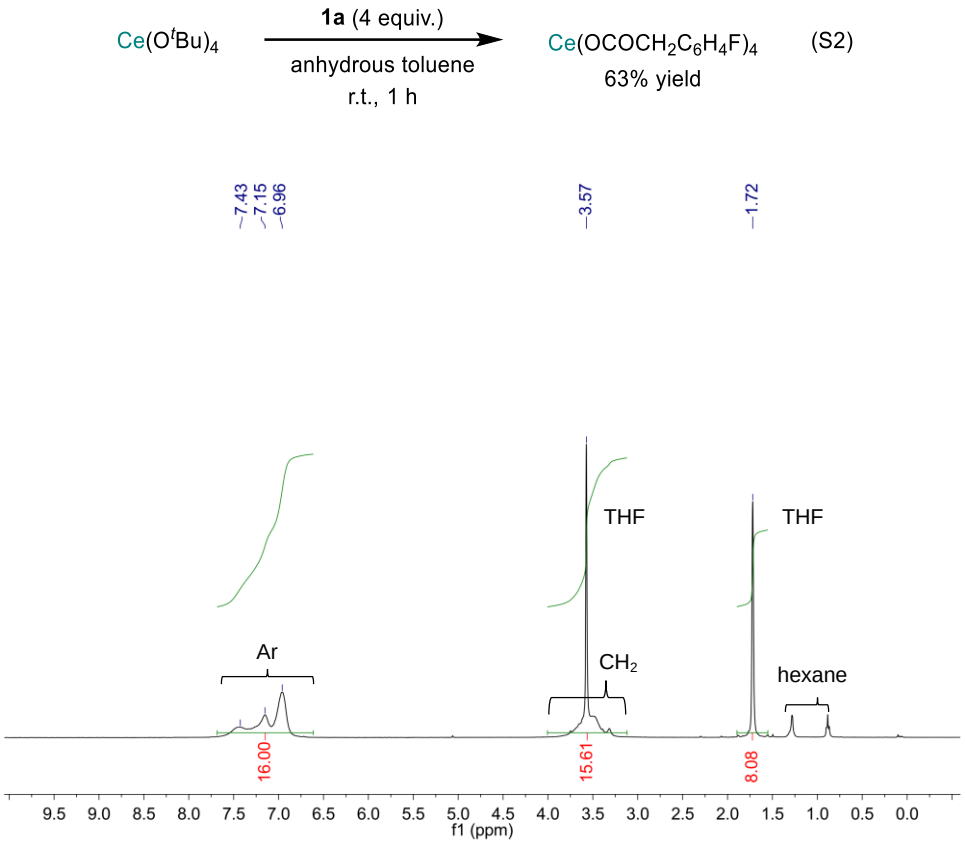

Figure S4. ^{1}H NMR spectrum of Ce(OCOCH$_2$C$_6$H$_4$F)$_4$ in THF-d_8 (400 MHz, 303K).

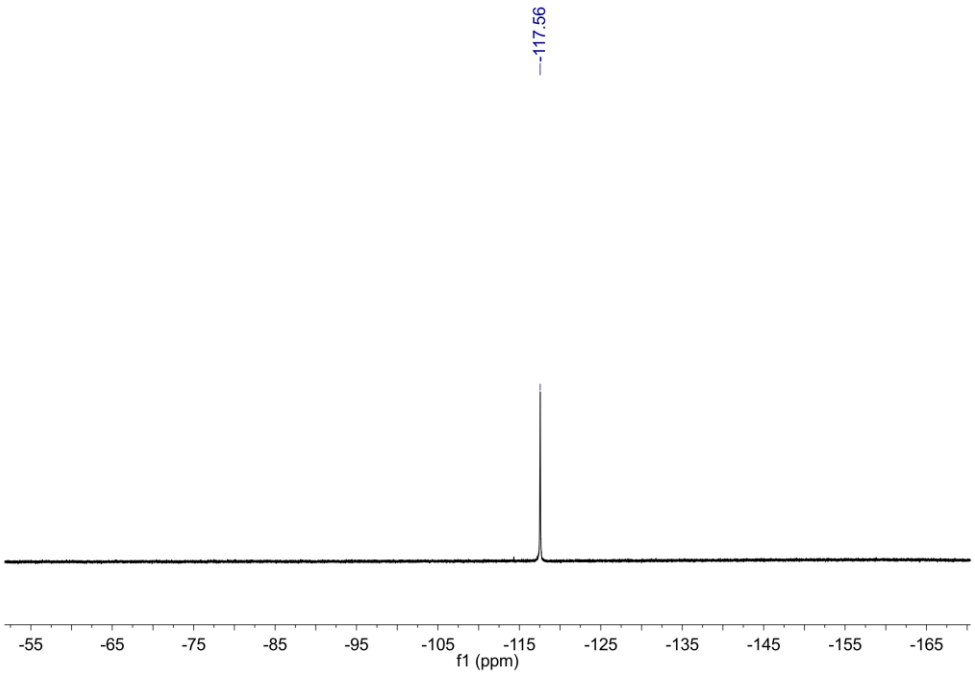

Figure S5. ^{19}F NMR spectrum of $Ce(OCOCH_2C_6H_4F)_4$ in THF-d_8 (400 MHz, 303K).

VI. Oxo-cerium Carboxylate Cluster Formation from $Ce(OCOCH_2C_6H_4F)_4$

To an orange powder of $Ce(OCOC_6H_4F)_4$ (3.8 mg, 0.100 mmol) was added 1.5 mL of toluene at room temperature to give a yellow solution. We detected hexanuclear cerium(IV) cluster-derived signals assignable as $\{[\mathbf{5}]\text{-}H^+\}^-$ and $\{[\mathbf{5}]_2\text{-}2H^+\}^{2-}$ ($\mathbf{5}$ = $Ce_6O_4(OH)_4(OCOCH_2C_6H_4F)_{12}$) in the ESI-MS spectrum (eq S3, Figure S6).

$$Ce(OCOCH_2C_6H_4F)_4 \xrightarrow[\text{r.t.}]{\text{toluene}} \underset{\mathbf{5}}{Ce_6O_4(OH)_4(OCOCH_2C_6H_4F)_{12}} \qquad \text{(S3)}$$

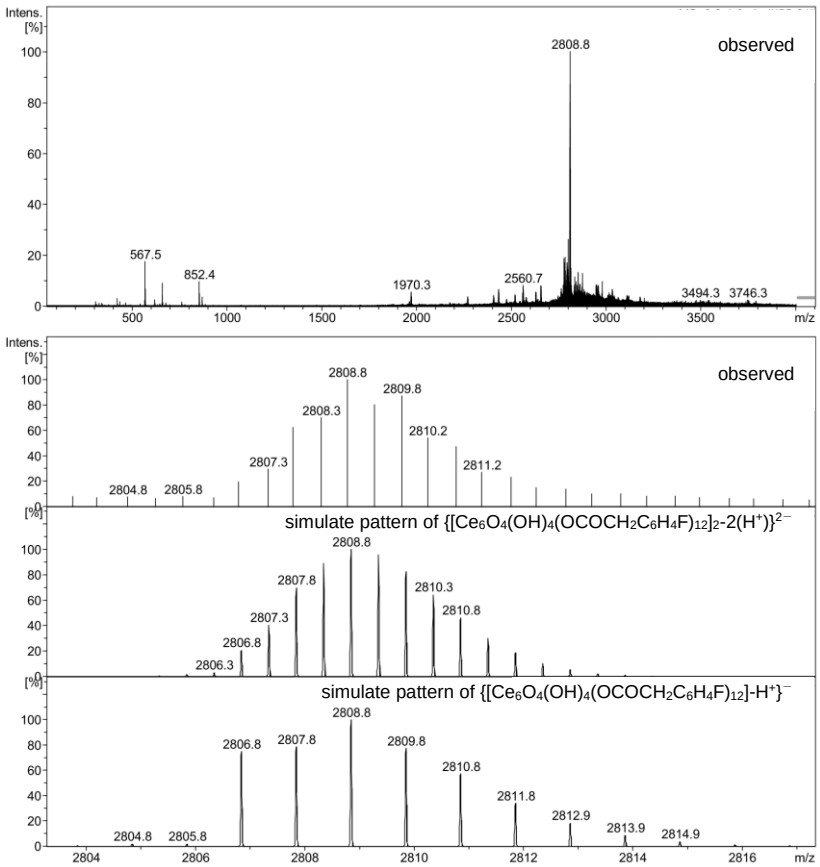

Figure S6. ESI-MS spectra of the mixture of $Ce(OCOCH_2C_6H_4F)_4$ in toluene at negative mode.

VII. Preparation of $Ce_6O_4(OH)_4(OCOCH_2{}^tBu)_{12}(HOCOCH_2{}^tBu)_4$ (6)

Following reaction was conducted under aerobic condition. To a yellow powder of $Ce(O{}^tBu)_4$ (150.0 mg, 0.347 mmol) in a screw vial was added a colorless solution of *tert*-butylacetic acid (408.0 mg, 3.51 mmol) in 3 mL of toluene at room temperature. A resulting yellow solution was stirred at room temperature for 12 h (eq S4). The reaction mixture was concentrated under reduced pressure, from which yellow crystals were precipitated. The crystals were isolated from the mixture by decantation and washed with cold toluene (0.2 mL x 3). $Ce_6O_4(OH)_4(OCOCH_2{}^tBu)_{12}(HOCOCH_2{}^tBu)_4$ (**6**) was obtained after drying under reduced pressure (92.0 mg, 56% yield). m.p. 109 °C (dec). ESI-MS (negative): m/z = 2353.4 ($[Ce_6O_4(OH)_4(OCOCH_2{}^tBu)_{12} - (H^+)]^-$). ^{1}H NMR (400 MHz, CD_2Cl_2, 303 K): δ 1.02 (br, 144 H), 2.05 (br, 32 H), 7.06 (br, 4H), 10.93 (br, 4H). $^{13}C\{^1H\}$ NMR (100 MHz, CD_2Cl_2, 303 K): δ 30.2 (CH_3), 30.8 (CH_2), 49.8 ($C(CH_3)_3$). Anal. calcd for $Ce_6O_4(OH)_4(OCOCH_2{}^tBu)_{12}(HOCOCH_2{}^tBu)_4$: $Ce_6C_{96}H_{184}O_{40}$: C, 40.90; H, 6.58. Found C, 40.06; H, 6.34. Deviation from the elemental analysis is probably due to the small contamination of $Ce_6O_4(OH)_4(OCOCH_2{}^tBu)_{12}(HOCOCH_2{}^tBu)_3(H_2O)$ in the sample.

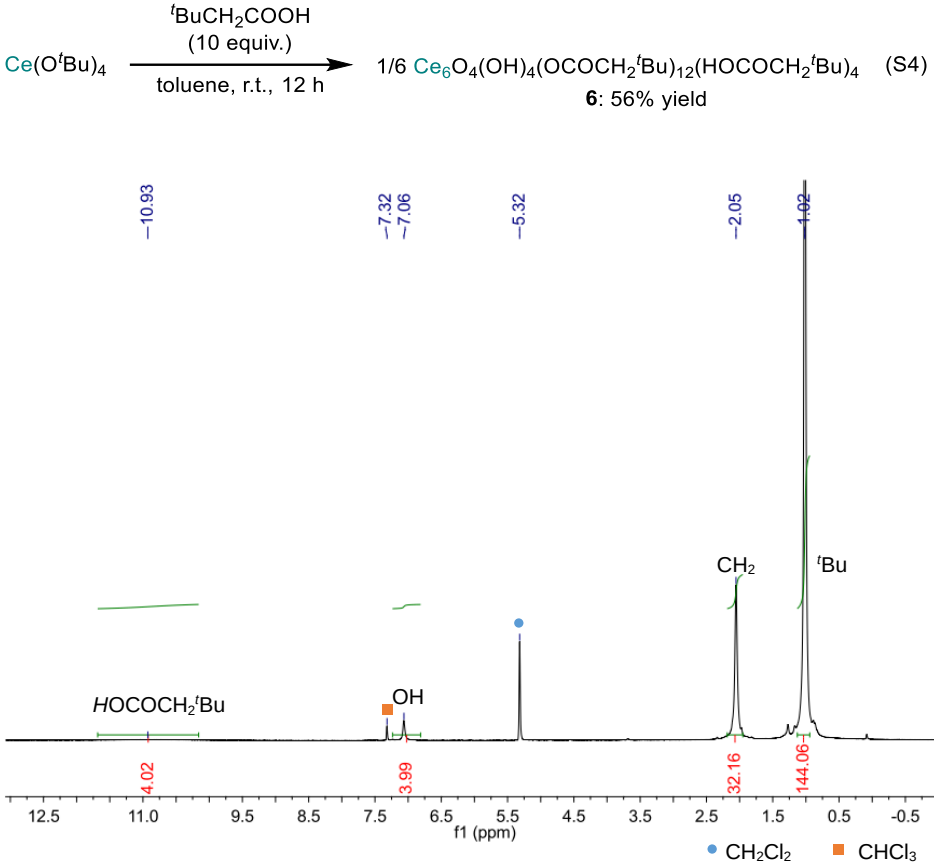

Figure S7. ^{1}H NMR spectrum of **6** in CD_2Cl_2 (400 MHz, 303K).

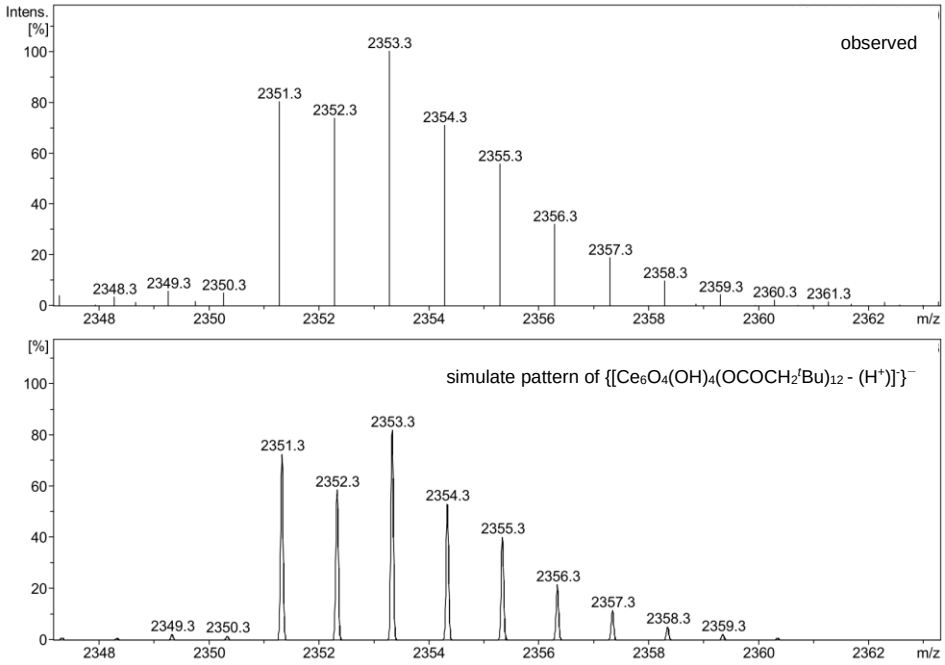

Figure S8. ESI-MS spectra of **6** in toluene at negative mode.

VIII. UV-Vis Spectrum of 6

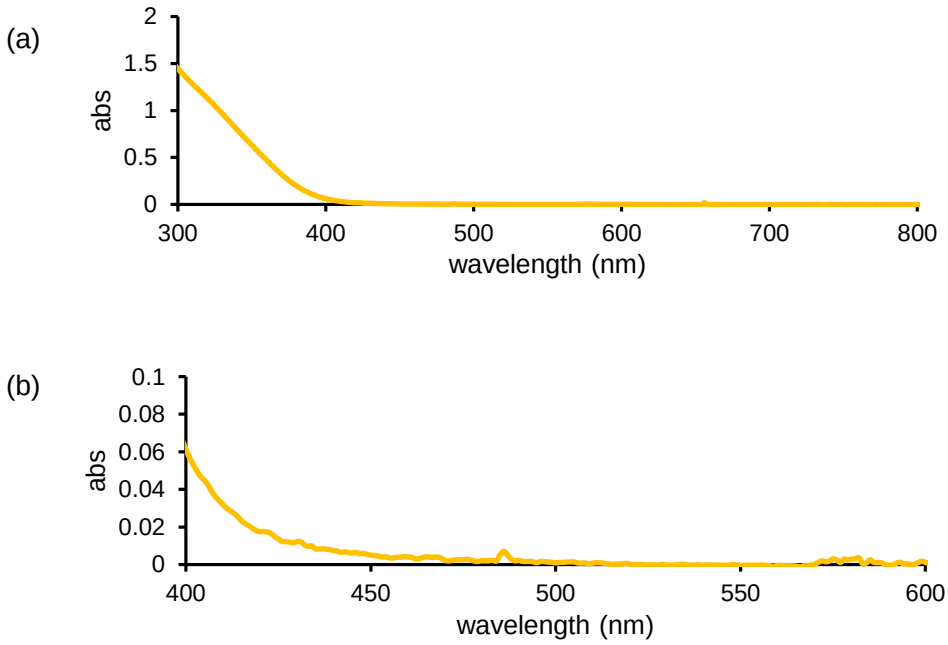

Figure S9. UV-vis spectra of **6** in toluene (2.4 mM on Ce): (a) 300-800 nm, (b) 400-600 nm.

IX. VT-NMR Spectra of 6 in CD_2Cl_2

The ^{1}H NMR spectrum of **6** in CD_2Cl_2 displayed one broad signal centered at δ 2.05 due to the methylene moieties of both μ_2-η^1:η^1-carboxylates and κ^1-*O* coordinated carboxylic acids at room temperature, indicating that carboxylate ligands and carboxylic acids bound to the cerium center were rapidly exchanged in solution at room temperature. The broad signal assignable to 12 carboxylates and 4 carboxylic acids was de-coalesced at 203 K, and 2 broad signals at δ 1.85 and 2.12 were finally observed at an approximately 3:1 ratio at 183 K (Figure S10). Using WinDNMR software,[3] the observed coalescence was well simulated with a pair of signals A and B (δ_A 1.80, δ_B 2.15 ppm, integral ratio between A and B : 3/1) undergoing identical rates of exchange (Figure S11).

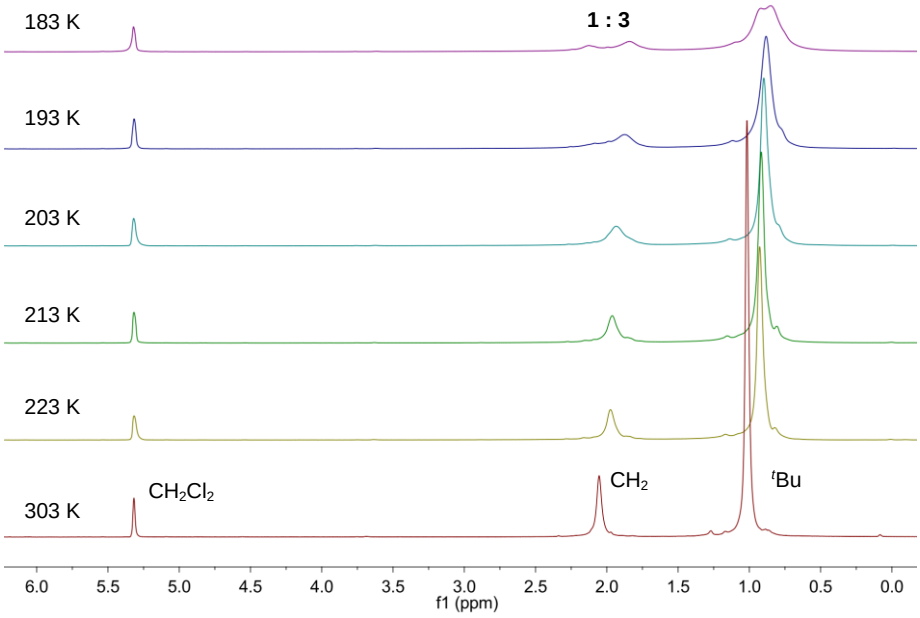

$$\Delta G^{\ddagger} = RTln\left(\frac{kT}{k_c h}\right), \qquad k_c = \frac{\pi}{\sqrt{2}}\Delta\nu_{AB}$$

$$\Delta G^{\ddagger}_{183} = 8.5 \text{ kcalmol}^{-1}, k_c = 256 \text{ s}^{-1}$$

Figure S10. ^{1}H VT-NMR spectra for **6** in CD_2Cl_2 between 183 K—303 K.

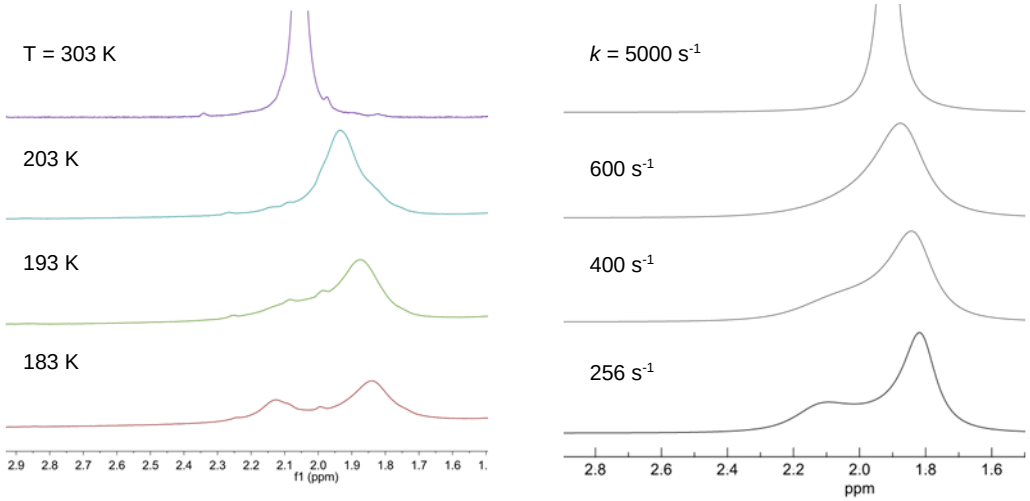

Figure S11. Experimental (left) and simulated (right) ^{1}H NMR spectra of the methylene resonances of carboxylic acids and carboxylates of **6** at various temperatures and rates of exchange; simulation parameters: δ_A 1.80 ppm, δ_B 2.15 ppm, $W_A = W_B = 0.33$ ppm, integral ratio of A and B, 3/1.

X. Photo-reduction of 6 with Blue LEDs (380−530 nm)

When the solution of **6** (0.0036 mmol) in toluene-d_8 (0.5 mL) in the presence of excess (30 equiv with respect to **6**) of ^{t}BuCH$_2$COOH was irradiated with blue LEDs for 1 hour *under argon atmosphere*, one of two *tert*-butyl carboxylate ligands bound to each Ce(IV) ion of **6** was photochemically activated to quantitatively give 2,2,5,5-tetramethylhexane (3 equiv with respect to **6**) as a consecutive decarboxylation and radical coupling product, along with formation of white precipitates of [Ce(OCOCH$_2$^{t}Bu)$_3$]$_n$ (**7a-7c** (n = 1-3)) (eq S5). The formula of **7** was determined by ESI-MS analysis (Figure S12). The photo-reduction process was also checked by ESI-MS analyses of the reaction mixture: before blue LEDs-irradiation of the reaction mixture, $Ce_6O_4(OH)_4(OCOCH_2{}^tBu)_{12}$ ([$Ce_6O_4(OH)_4(OCOCH_2{}^tBu)_{12}$-H$^+$]$^-$: *m*/*z* = 2353.3) was detected along with other oxo-cerium(IV) carboxylates such as [$Ce_6O_8(OCOCH_2{}^tBu)_8$][$Ce_n(OCOCH_2{}^tBu)_{4n}$] (n = 1, {[$Ce_6O_8(OCOCH_2{}^tBu)_8$][Ce(OCOCH$_2$^{t}Bu)$_4$](^{t}BuCH$_2$CO$_2$H)$_2$-H$^+$}$^-$: *m*/*z* = 2721.4; n = 2, {[$Ce_6O_8(OCOCH_2{}^tBu)_8$][$Ce_2(OCOCH_2{}^tBu)_8$]+(e$^-$)}$^-$: *m*/*z* = 3091.5) (Figure S13), while no signal assignable to the cerium clusters was observed after irradiation, indicating that Ce(IV) carboxylate cluster **6** was reduced by the irradiation (Figure S14).

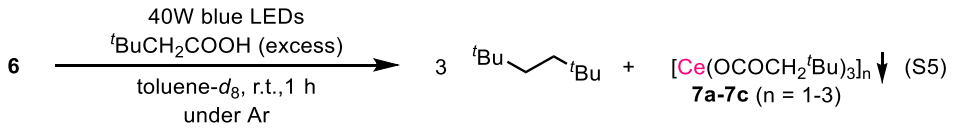

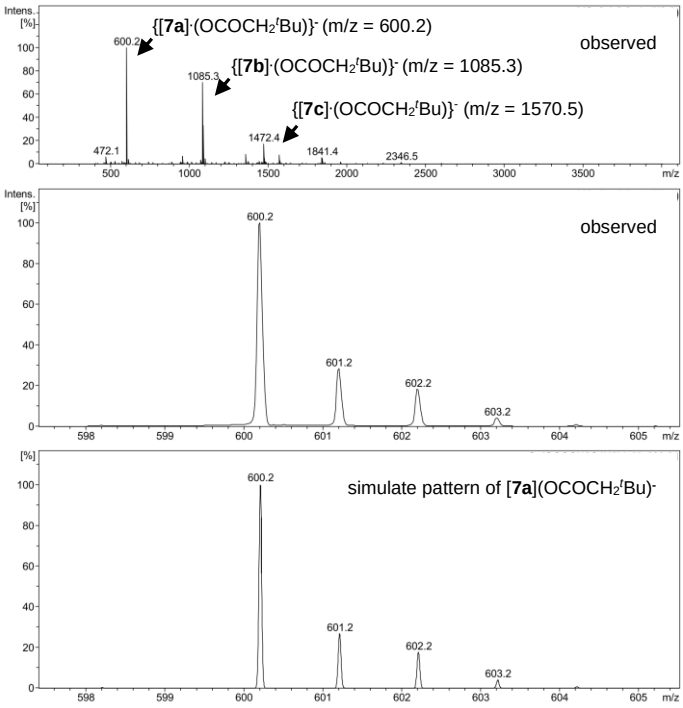

Figure S12. ESI-MS spectra of white precipitate of [$Ce_n(OCOCH_2{}^tBu)_{3n}$] (**7a** : n =1, **7b** : n = 2, **7c** : n = 3) in MeOH at negative mode.

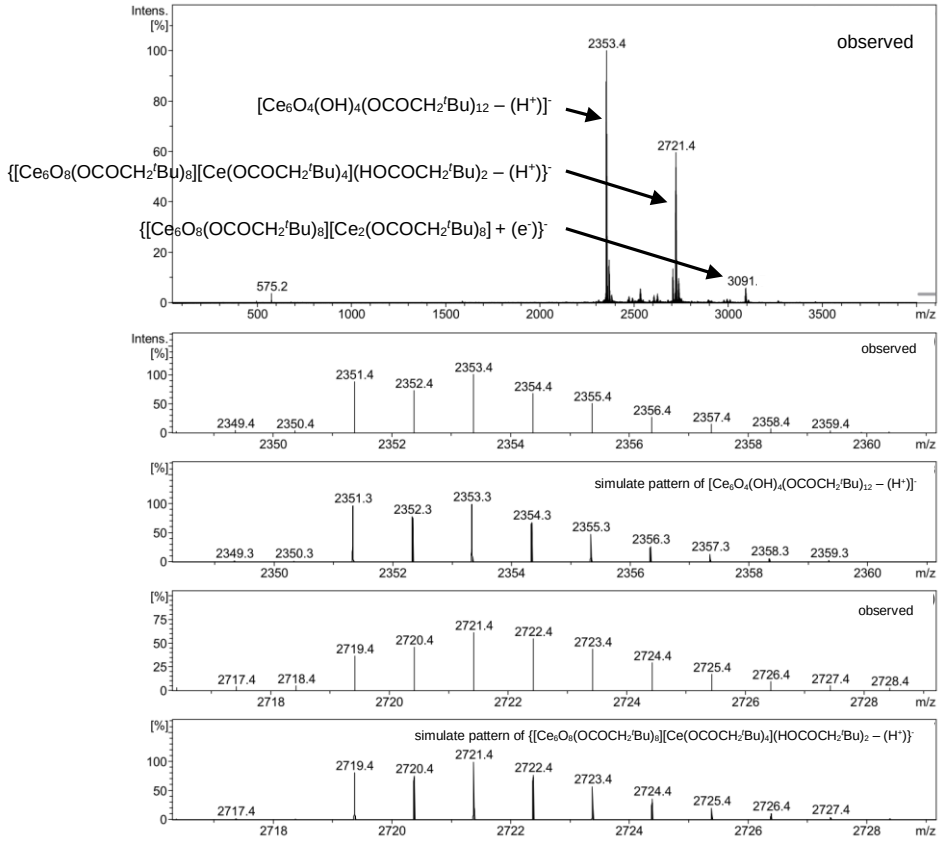

Figure S13. ESI-MS spectra of reaction mixture of **6** in the presence of excess of ^{t}BuCH$_2$COOH at negative mode (before blue LEDs irradiation).

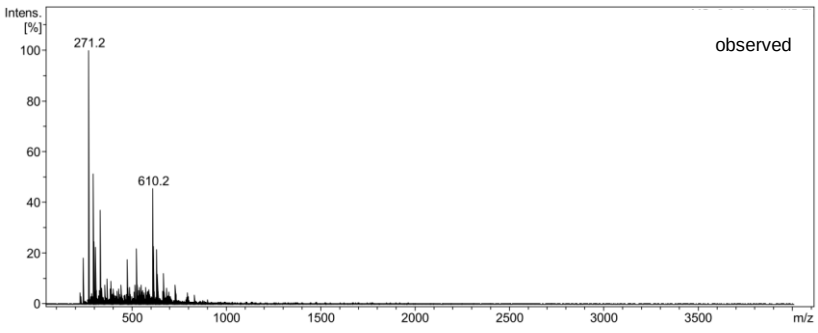

Figure S14. ESI-MS spectrum of reaction mixture of **6** in the presence of excess of ^{t}BuCH$_2$COOH after 1 h irradiation by blue LEDs at negative mode.

XI. Observation of Cerium(IV) Alkylperoxo Species

When the mixture of $Ce(O^tBu)_4$ (0.010 mmol) and excess (10 equiv) of 2-(trifluoromethyl)phenylacetic acid in toluene (1.5 mL) was irradiated with blue LEDs for 10 minutes, we observed reduced cerium(III) species, $[Ce(OCOCH_2C_6H_4CF_3)_3]_n$ (n = 1, $\{[Ce(OCOCH_2C_6H_4CF_3)_3](OCOCH_2C_6H_4CF_3)\}^-$: *m/z* = 952.0; n = 2, $\{[Ce_2(OCOCH_2C_6H_4CF_3)_6](OCOCH_2C_6H_4CF_3)\}^-$: *m/z* = 1701.0) as main species and trace amounts of cerium(IV) alkylperoxo species, $Ce_2O(OCOCH_2C_6H_4CF_3)_5(OOCH_2C_6H_4CF_3)$ (**8**) ($\{$**[8]**$(CH_3CN)(OH)\}^-$: *m/z* = 1560.0) by ESI-MS analysis (eq S6, Figure S15).

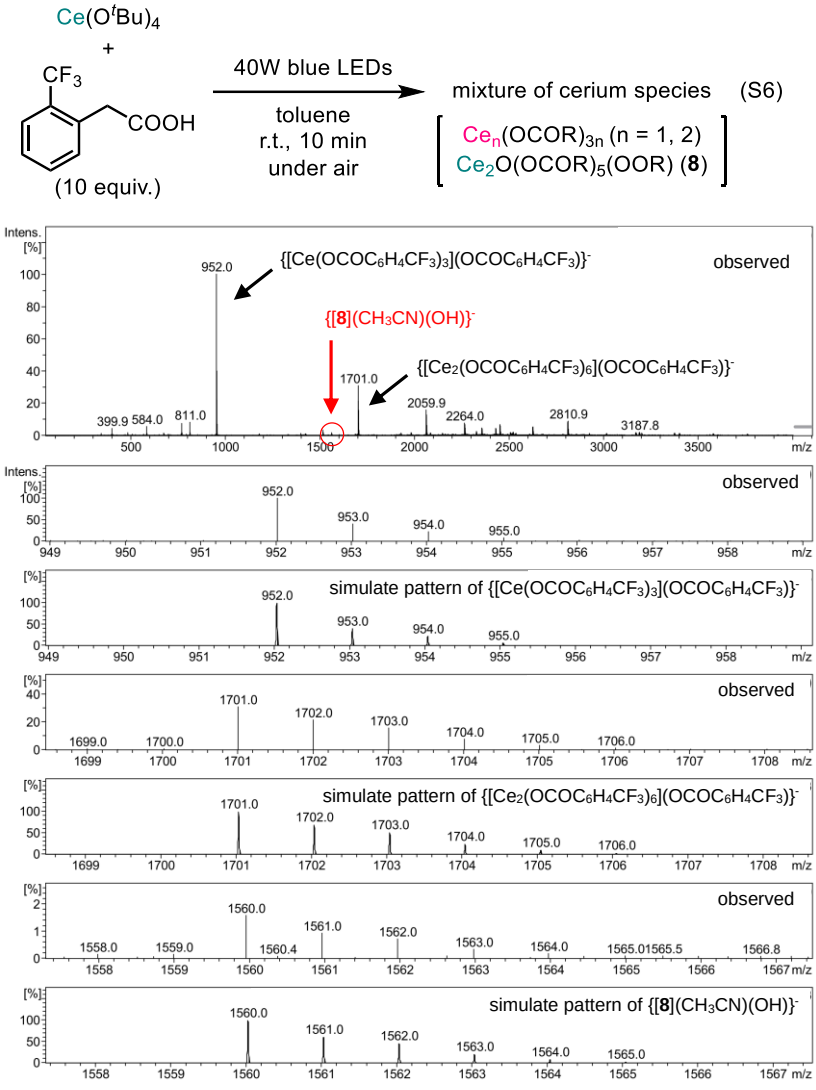

Figure S15. ESI-MS spectra of the reaction mixture of $Ce(O^tBu)_4$ and excess (10 equiv) of 2-(trifluoromethyl)phenylacetic acid in toluene after 10 min irradiation of blue LEDs at negative mode. The sample was diluted with CH_3CN for the measurement.

XII. Reaction Progress for the Decarboxylative Oxygenation of 1a

Amounts of the products **2a-4a** were calculated by following the reaction progress in every 1 hour under the optimized reaction conditions (Figure S16). Initially, 4-fluorobenzyl hydroperoxide (**4a**) was formed in 1 h, and **4a** was gradually decomposed to give a mixture of 4-fluorobenzaldehyde (**2a**) and 4-fluorobenzyl alcohol (**3a**) in the following reaction time, which is consistent with the typical decomposition of organic hydroperoxides under oxidation condition.[4] *In situ*-generated carbon radicals were trapped by O_2 to produce alkyl hydroperoxides, and subsequent decomposition of the peroxides gave a mixture of aldehydes and alcohols. It is important to note that no conversion of **3a** to **2a** was observed under the reaction condition, indicating that **2a** was produced *via* decomposition of **4a**, not *via* cerium-catalyzed dehydrogenative oxidation of **3a**. In addition, we found significant acceleration on the rate of decomposition for **4a** at the end of the catalytic reaction.

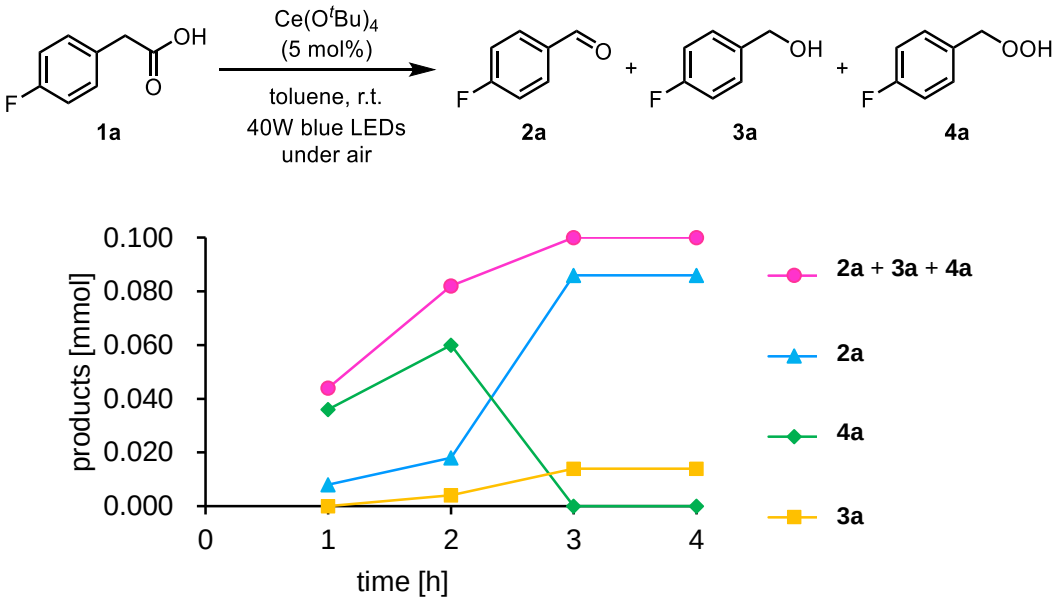

Figure S16. Reaction trace of the decarboxylative oxygenation of **1a**. Reaction conditions: **1a** (0.100 mmol), Ce(O^{t}Bu)$_4$ (5 mol%), toluene (1.5 mL), under air, 40W blue LEDs, 1,3,5-trimethoxybenzene as an internal standard.

XIII. Optimization of Reaction Conditions for Lactonization of 9

To catalysts placed in a test tube (size: φ 13 mm x 105 mm) was added a mixture of **9** (0.100 mmol) and 1,3,5-trimethoxybenzene as an internal standard in toluene (1.5 mL). The reaction mixture was irradiated with 40W blue LEDs with stirring at room temperature under air for 6 h. For determining their yields by ^{1}H NMR measurement, a portion of the reaction mixture was diluted with $CDCl_3$, and signal intensities due to the methyl hydrogens of **10** and **11** were calculated with respect to the internal standard.

Table S4. Screening of Metal Catalysts[a,b]

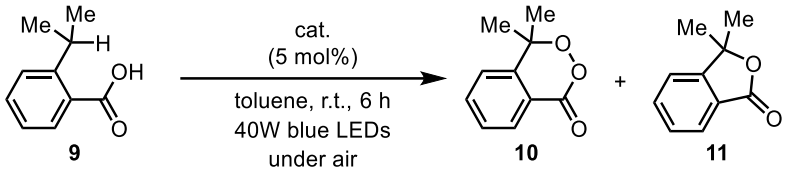

entry	cat.	yield (%) of **10**	yield (%) of **11**
1	$Ce(O^tBu)_4$	69	27
2	$Ce_6O_4(OH)_4(OCOCH_2{}^tBu)_{12}(HOCOCH_2{}^tBu)_4$ (**6**)	79	20
3	$Fe(OAc)_2$	n.d.	21
4[c]	$Fe(OAc)_2$	n.d.	28
5	$Fe(OH)(OAc)_2$	n.d.	14
6	$Fe(acac)_3$	n.d.	6
7	$Co(OAc)_2$	trace	trace
8	$Co(acac)_2{\cdot}2H_2O$	n.d.	n.d.
9	$Co(acac)_3$	n.d.	n.d.
10	$Mn(acac)_2{\cdot}2H_2O$	n.d.	n.d.
11	$Mn(OAc)_3{\cdot}2H_2O$	trace	trace
12	$Cu(OAc)_2{\cdot}2H_2O$	trace	n.d.

[a] NMR yields. [b] Reaction conditions: **1a** (0.100 mmol), cat. (5 mol%), toluene (1.5 mL), under air, 40W blue LEDs, 1,3,5-trimethoxybenzene as an internal standard. [c] 48 h.

Table S5. Screening of Co-catalyst[a,b]

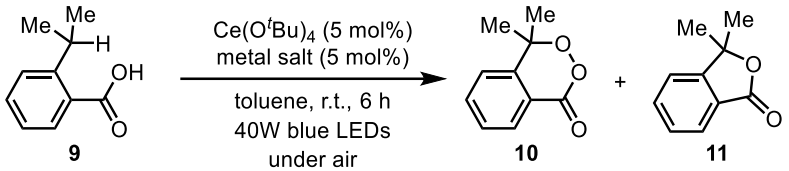

entry	metal salt	yield (%) of **10**	yield (%) of **11**	**10** : **11**
1	none	69	27	1 : 0.33
2	$Co(OAc)_2$	49	48	1 : 0.98
3	$Co(acac)_2{\cdot}2H_2O$	41	55	1 : 1.4
4[c]	$Co(acac)_2{\cdot}2H_2O$	34	42	1 : 1.2
5[d]	$Co(acac)_2{\cdot}2H_2O$	9	91	1 : 10
6	$Mn(OAc)_3{\cdot}2H_2O$	51	23	1 : 0.44
7	$Mn(acac)_2{\cdot}2H_2O$	42	38	1 : 0.90
8	$Cu(OAc)_2{\cdot}2H_2O$	45	5	1 : 0.13
9	$Fe(OAc)_2$	77	21	1 : 0.28
10	$Fe(acac)_3$	18	7	1 : 0.4

[a] NMR yields. [b] Reaction conditions: **1a** (0.100 mmol), Ce(O^{t}Bu)$_4$ (5 mol%), metal salt (5 mol%), toluene (1.5 mL), under air, 40W blue LEDs, 1,3,5-trimethoxybenzene as an internal standard. Reaction vessel : test tube (φ = 13 mm). [c] Glass Schlenk (φ = 28 mm) was used as a reaction vessel. [d] Glass Schlenk (φ = 7.4 mm) was used as a reaction vessel.

For this bimetallic catalyst system, a vessel with smaller surface area increased the amount of **10** (Table S5, entry 3-5), because low concentration of O_2 in the reaction mixture suppressed the oxygenation of *in situ*-generated carbon radical.

XIV. Isolation of Peroxy Lactone 10

To $Ce(O^tBu)_4$ (1 mol%) placed in a test tube (size: φ 15 mm x 130 mm) was added a mixture of **9** (0.300 mmol) and 1,3,5-trimethoxybenzene as an internal standard in toluene (1.5 mL). The reaction mixture was irradiated with 40W blue LEDs with stirring at room temperature under air for 6 h. A resulting mixture of **10** (91% yield) and **11** (9% yield) was quenched with 1 M HCl aq. and **11** was extracted with diethyl ether. The remaining water layer was quenched with saturated $NaHCO_3$ aq. and **10** was extracted with diethyl ether and dried under reduced pressure. **10** was purified by silica gel flush column chromatography (hexane/ethyl acetate = 19/1).

Compound data of **10**: ^{1}H NMR (400 MHz, $CDCl_3$, 30 °C): δ 1.69 (s, 6H), 7.25 (d, *J* = 7.2 Hz, 1H), 7.64 (td, *J* = 7.2, 1.1 Hz, 1H), 7.64 (td, 7.9, *J* = 1.1 Hz, 1H), 8.14 (d, *J* = 7.9 Hz, 1H). ^{13}C NMR (100 MHz, $CDCl_3$, 30 °C): δ 25.1, 82.7, 120.3, 122.7, 128.2, 130.3, 134.9, 146.7, 167.1. HRMS (EI) (*m*/*z*) : $[M]^+$ calcd. for $C_{10}H_{10}O_2$ 178.0630; found 178.0631. IR (KBr, *ν*/cm^{-1}): 3448 br m, 2987 m, 2918 m, 2850 m, 1753 s, 1738 s, 1285 s, 1248 m, 1100 m, 1058 m, 1031 w, 762 m, 693 m.

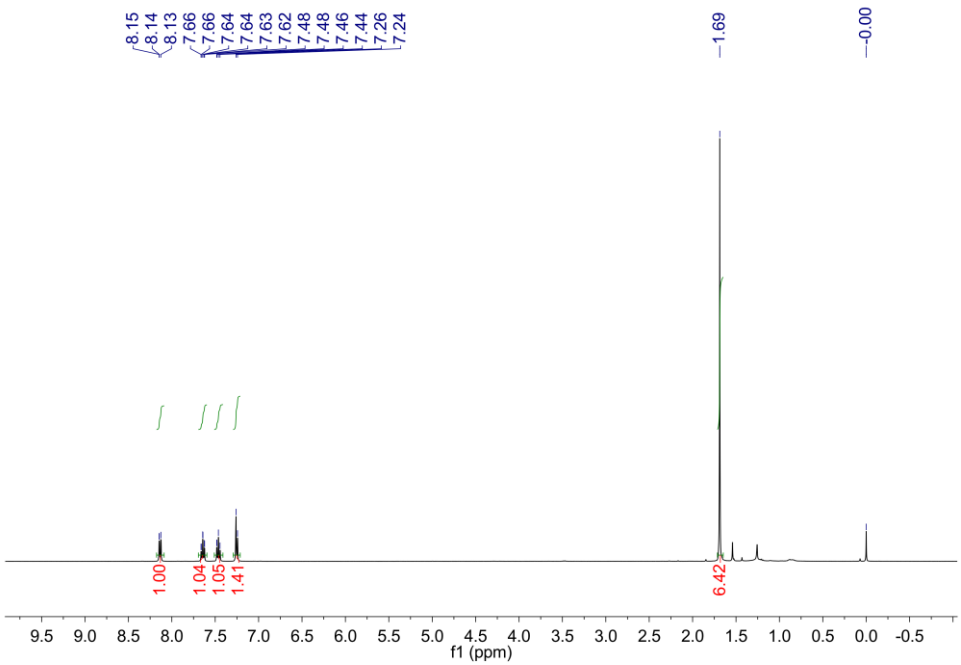

Figure S17. ^{1}H NMR spectrum of **10**.

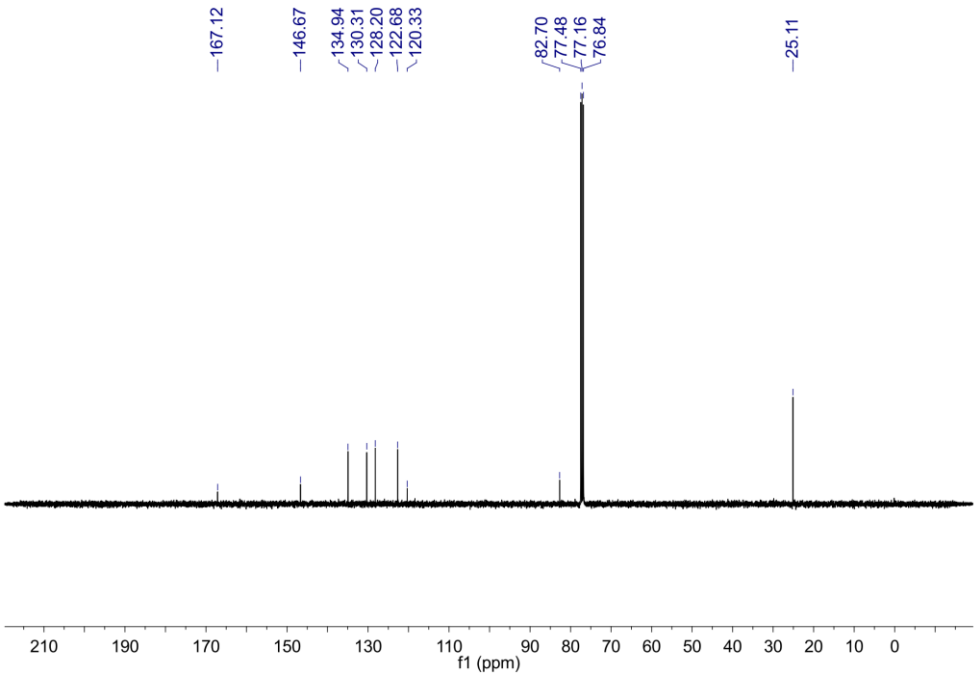

Figure S18. ^{13}C NMR spectrum of **10**.

XV. ESI-MS Spectra of the Mixture of $Ce(O^tBu)_4$ and 9 in Toluene

A colorless solution of **9** (0.100 mmol) in 1.5 mL of toluene was added to $Ce(O^tBu)_4$ (0.010 mmol) at room temperature to give yellow solution of oxo cerium carboxylate clusters including a tetranuclear oxo cerium carboxylate, $Ce_4O_2(OCOC_9H_{11})_{12}$, confirmed by the observation in ESI-MS ($[Ce_4O_2(OCOC_9H_{11})_{12}+(e^-)]^-$: *m/z* = 2550.5) (eq S7, Figure S19). After 10 minutes blue LEDs-irradiation of the mixture, cerium(III) carboxylates, $Ce_n(OCOC_9H_{11})_{3n}$, were detected by ESI-MS (Figure S20).

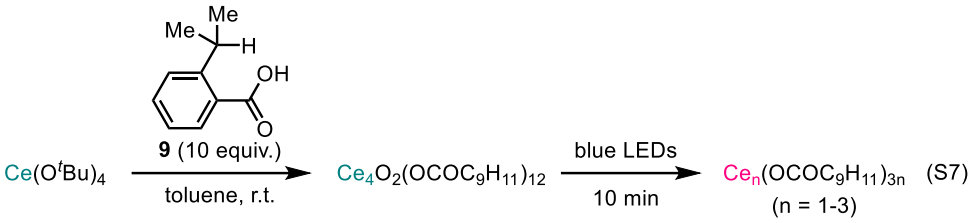

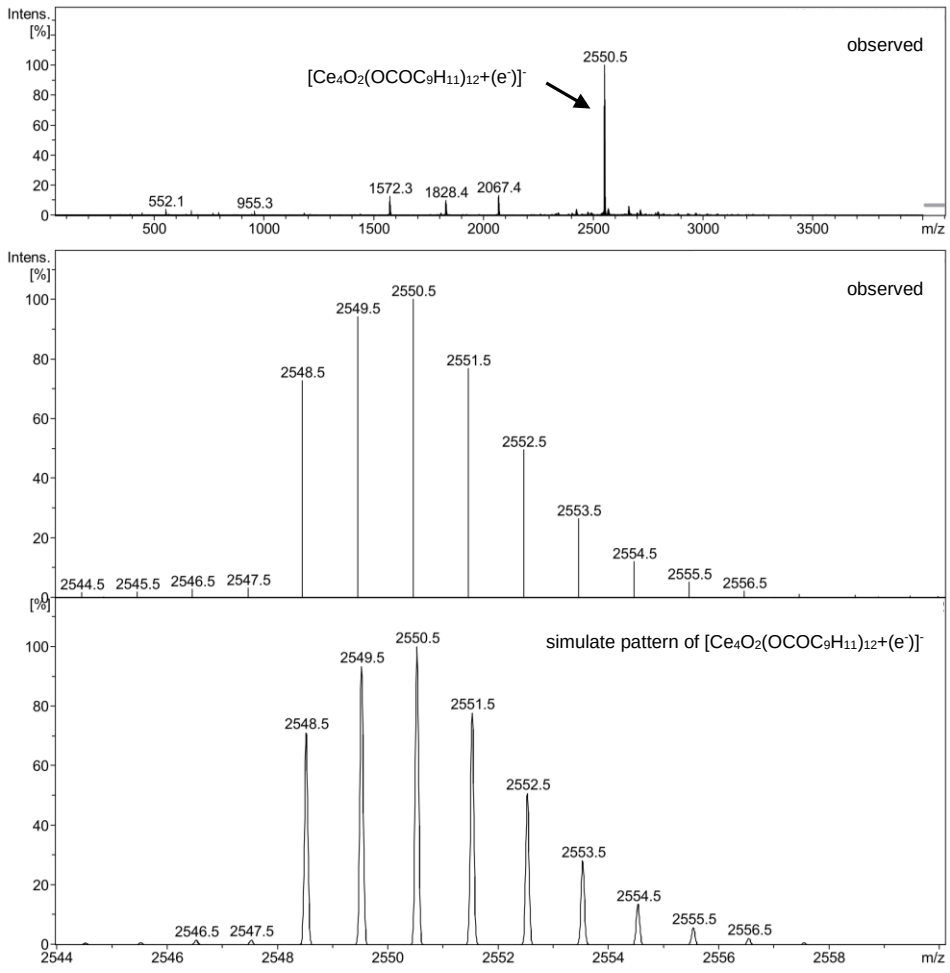

Figure S19. ESI-MS spectra of the mixture of $Ce(O^tBu)_4$ and 10 equiv of **9** in toluene at negative mode.

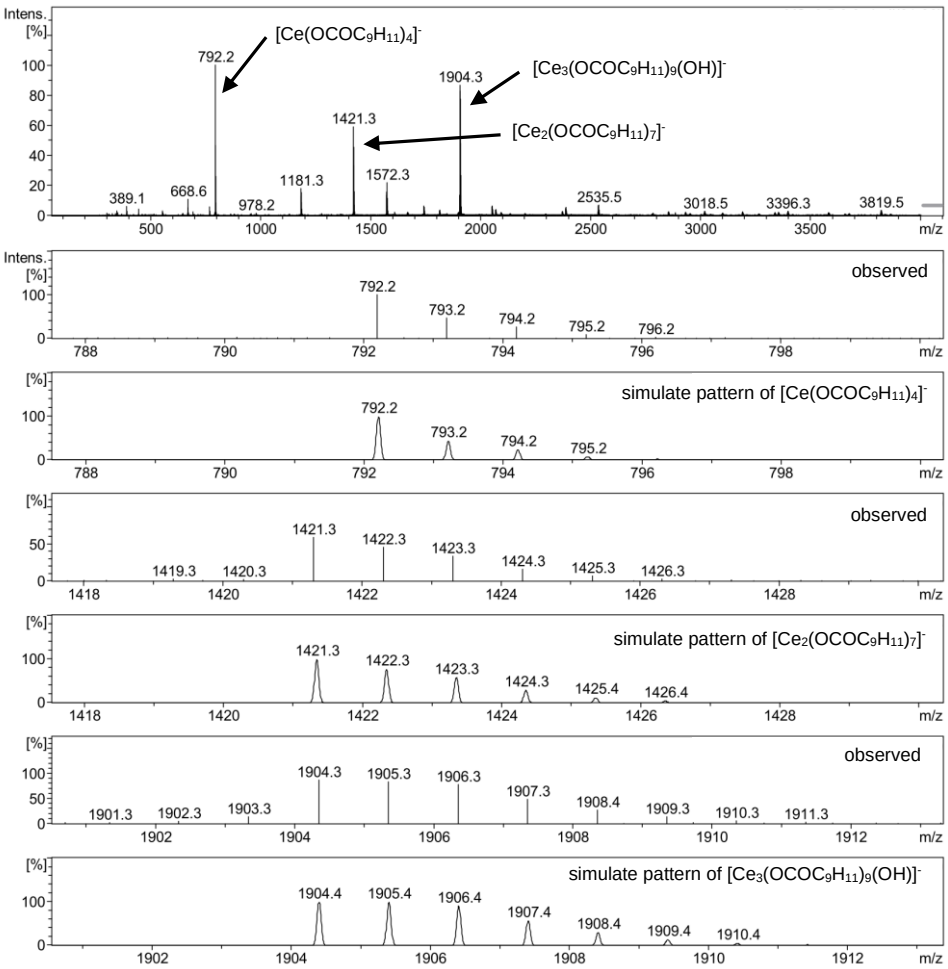

Figure S20. ESI-MS spectra of the mixture of $Ce(O^tBu)_4$ and 10 equiv of **9** in toluene after irradiation for 10 min by blue LEDs at negative mode.

XVI. ESI-MS Spectra of the Mixture of $Ce(O^tBu)_4$, $Co(acac)_2{\cdot}2H_2O$ and 9 in Toluene

A purple solution of **9** (0.100 mmol) and $Co(acac)_2{\cdot}2H_2O$ (0.005 mmol) in 1.5 mL of toluene was added to a yellow powder of $Ce(O^tBu)_4$ (0.005 mmol) at room temperature to give yellowish green solution of oxo cerium carboxylate clusters including heterometallic oxo-cerium-cobalt carboxylates, $Ce_{1+n}CoO_n(OCOC_9H_{11})_{6+2n}$ (n = 1, $\{[Ce_2CoO(OCOC_9H_{11})_8](OCOC_9H_{11})\}^-$: *m/z* = 1822.4; n = 2, $\{[Ce_3CoO_2(OCOC_9H_{11})_{10}](OCOC_9H_{11})\}^-$: *m/z* = 2305.5; n = 3, $\{[Ce_4CoO_3(OCOC_9H_{11})_{12}](OCOC_9H_{11})\}^-$: *m/z* = 2788.5), and polynuclear oxo-cerium carboxylate clusters, $Ce_{2+n}O_n(OCOC_9H_{11})_{8+2n}$ (n = 1, $[Ce_3O(OCOC_9H_{11})_{10}+(e^-)]^-$: *m/z* = 2067.5; n = 2, $[Ce_4O_2(OCOC_9H_{11})_{12}+(e^-)]^-$: *m/z* = 2550.5), confirmed by ESI-MS (eq S8, Figure S21).

When we used monometallic cerium system, cerium(III) species was observed by ESI-MS after 10 minutes irradiation of blue LEDs (Figure S20, eq S7). On the other hands, in the case of using Ce/Co heterometallic system, no cerium(III) species were observed after 10 minutes irradiation of blue LEDs, but cerium(IV) species such as $Ce_{1+n}CoO_n(OCOC_9H_{11})_{6+2n}$, $Ce_{2+n}O_n(OCOC_9H_{11})_{8+2n}$ were observed (Figure S22). This result indicated that cobalt worked as an oxidant for regenerating cerium(IV) species, which oxidized *in situ*-generated carbon radical **E** to give carbocation **H** to form lactone **11** (Scheme 3, main text).

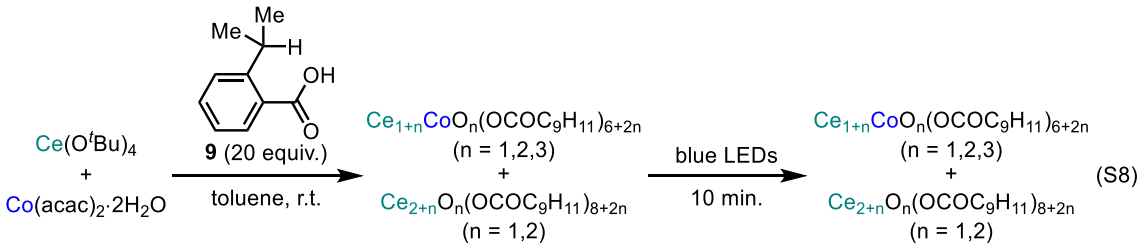

(S8)

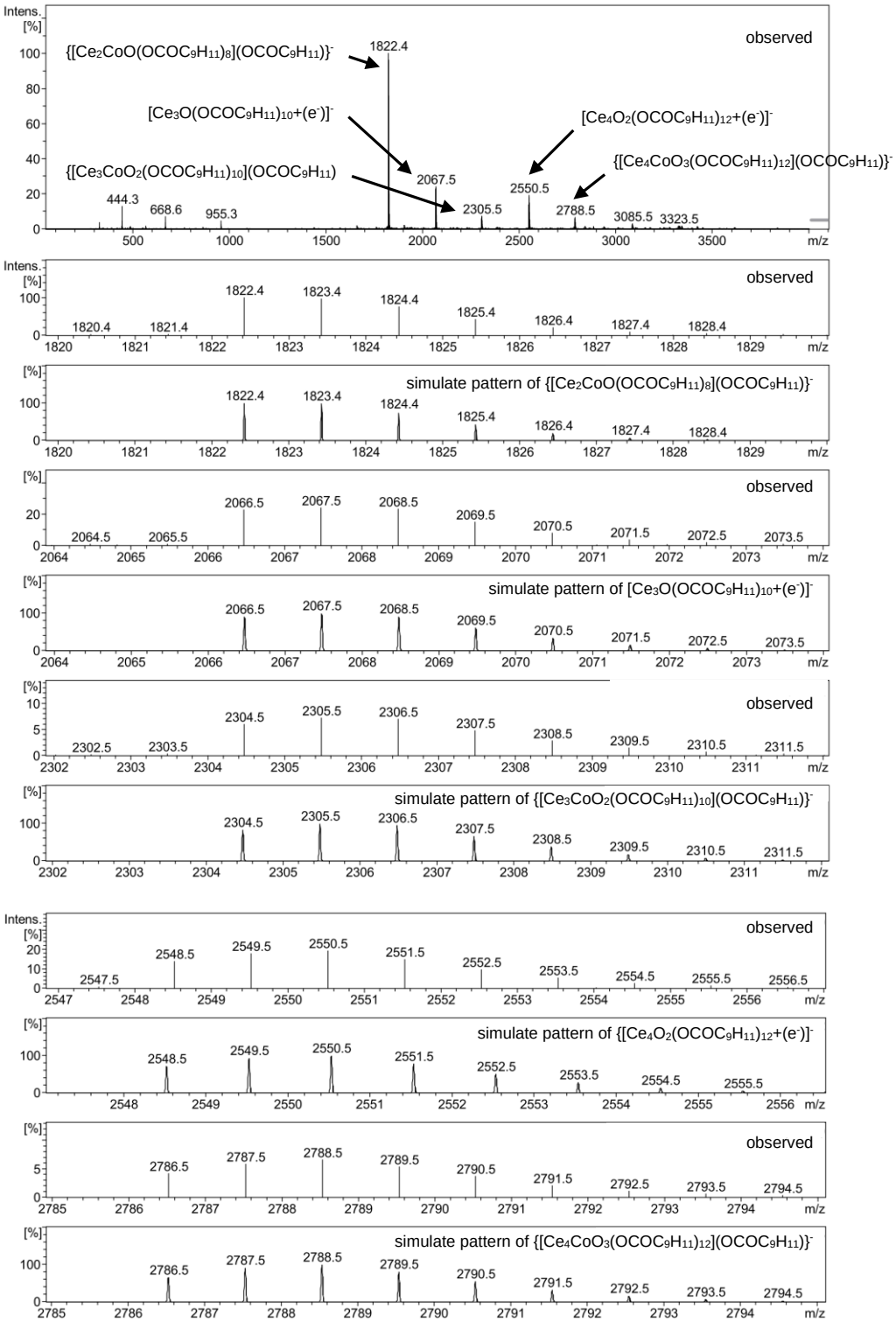

Figure S21. ESI-MS spectra of the mixture of $Ce(O^tBu)_4$, $Co(acac)_2{\cdot}2H_2O$ and 10 equiv of **9** in toluene at negative mode.

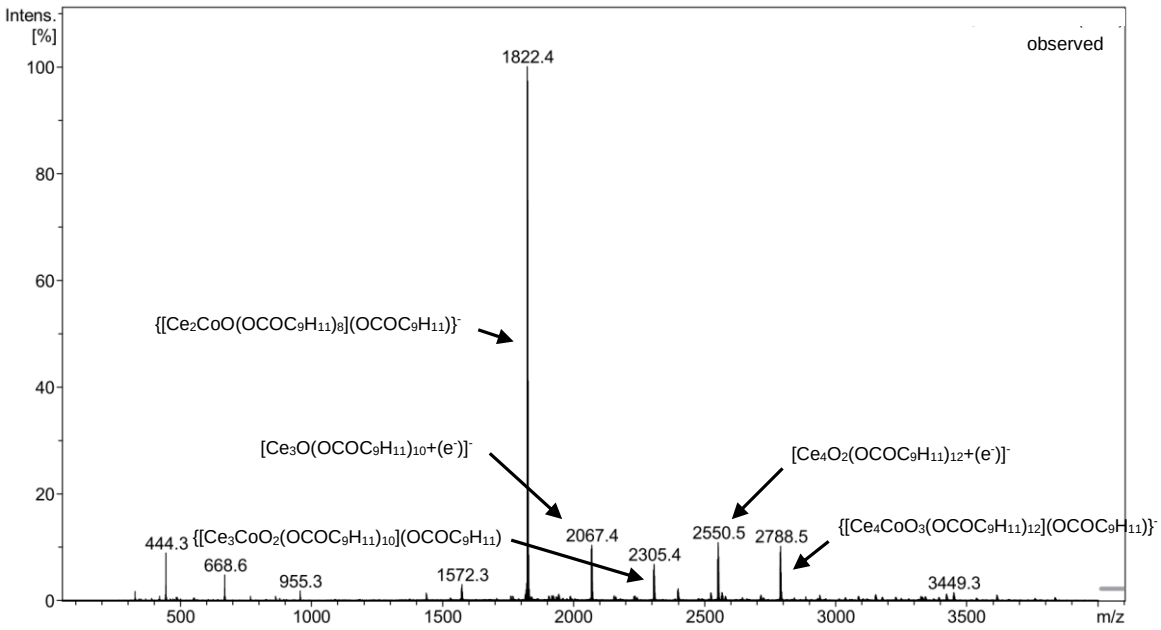

Figure S22. ESI-MS spectra of the mixture of $Ce(O^tBu)_4$, $Co(acac)_2 \cdot 2H_2O$ and 10 equiv of **9** in toluene after 10 minutes irradiation of blue LEDs at negative mode.

XVII. Labeling Experiments of Lactonization of 9

Lactonization of **9** was performed under 1.5 atm of $^{18}O_2$ (99%) instead of atmospheric air pressure under optimized reaction conditions to give [$^{18}O_2$]-**10**, **11**, [^{18}O]-**11**, [^{18}O]'-**11** and [$^{18}O_2$]-**11** (eq S9). The reaction mixture was quenched with EtOAc and the reaction mixture was filtered with silica gel and dried under reduced pressure. The NMR yield was determined by integral ratios of signals for triphenylmethane and methyl protons of **10** and **11**. The ^{18}O was determined by HRMS and GC-MS (Figure S23). Scheme S1 shows the possible reaction pathways for forming ^{18}O-containing lactones such as [^{18}O]-**11** and [$^{18}O_2$]-**11** *via* hydrolysis of **11** and [^{18}O]'-**11**.

HRMS (EI) (*m*/*z*) : [**10**]$^+$ calcd. for $C_{10}H_{10}O^{18}O_2$ 178.0715; found 182.0707.

HRMS (EI) (*m*/*z*) : [**11**]$^+$ calcd. for $C_{10}H_{10}O_2$ 162.0681; found 162.0679.

HRMS (EI) (*m*/*z*) : [[^{18}O]-**11**]$^+$ calcd. for $C_{10}H_{10}O^{18}O$ 164.0723; found 164.0715.

HRMS (EI) (*m*/*z*) : [[$^{18}O_2$]-**11**]$^+$ calcd. for $C_{10}H_{10}{}^{18}O_2$ 166.0766; found 166.0765.

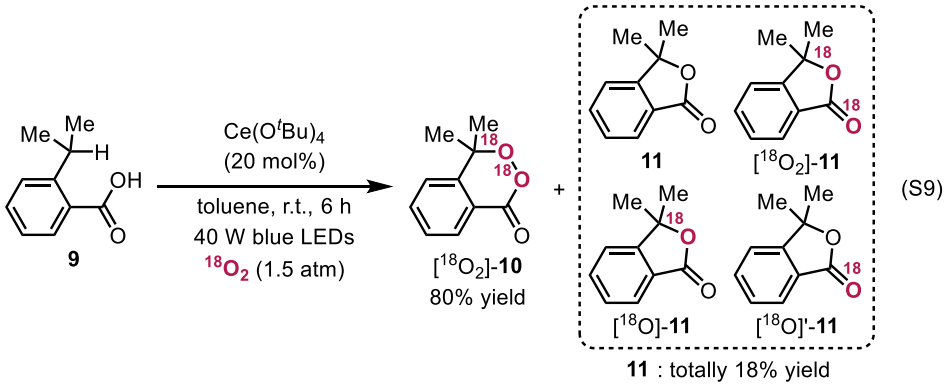

Scheme S1. **Possible Reaction Pathways for Forming ^{18}O-Containing Lactones**

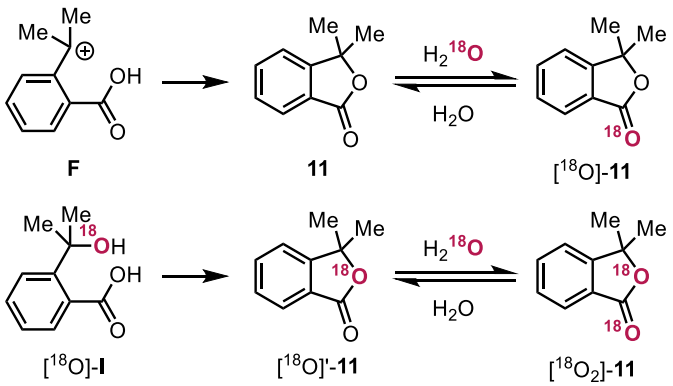

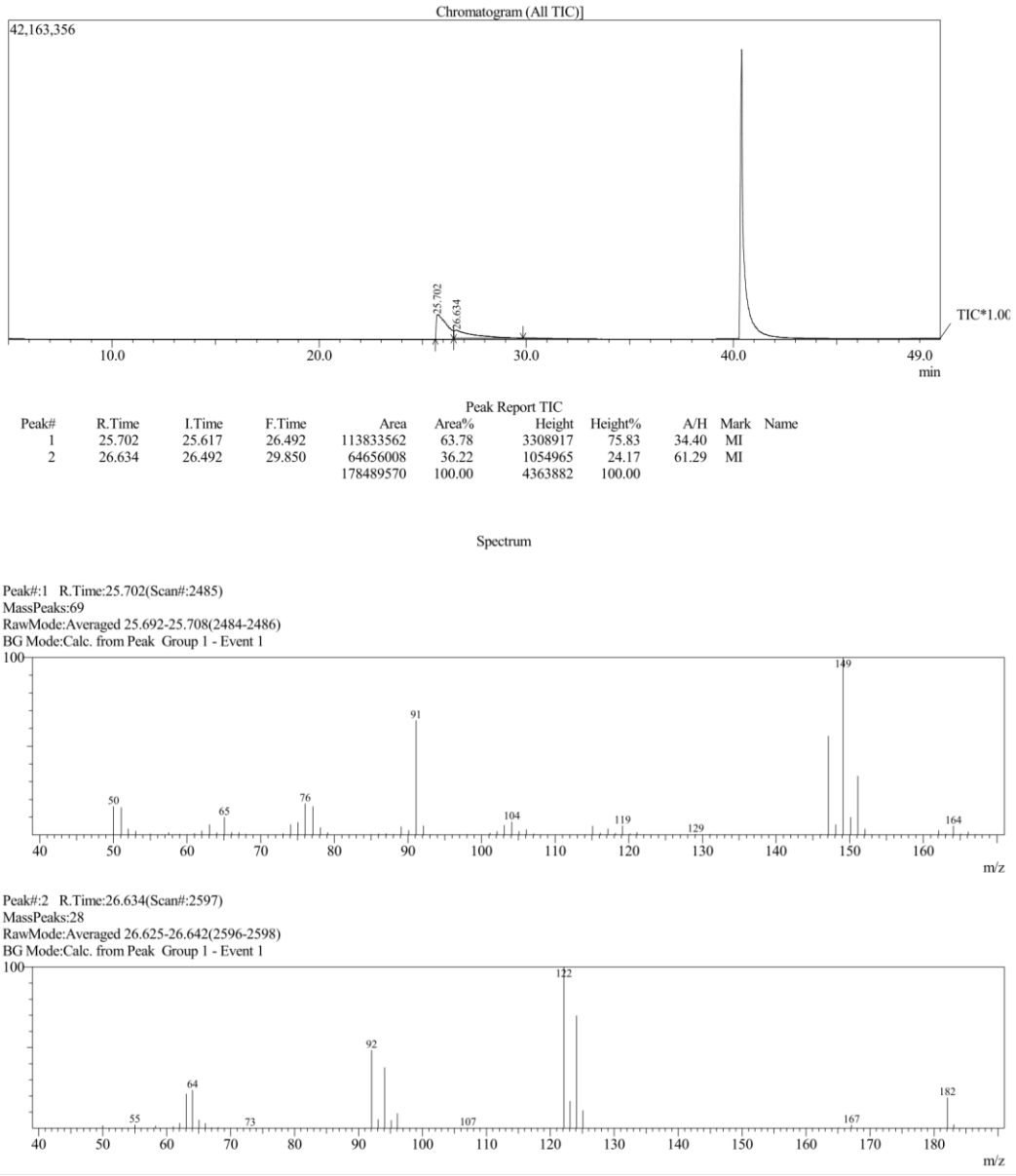

Peak Report TIC

Peak#	R.Time	I.Time	F.Time	Area	Area%	Height	Height%	A/H	Mark	Name
1	25.702	25.617	26.492	113833562	63.78	3308917	75.83	34.40	MI	
2	26.634	26.492	29.850	64656008	36.22	1054965	24.17	61.29	MI	
				178489570	100.00	4363882	100.00			

Spectrum

Figure S23. GC-MS Spectra of the reaction mixture of lactonization of **9** under $^{18}O_2$ (99%).

XVIII. Spectral Data

Formation of the decarboxylative oxygenated products was confirmed by comparing the corresponding commercially available aldehydes, ketones, and alcohols. The underlined signals were used for determining the yield in the ^{1}H NMR spectra. In some cases, small amounts of benzaldehyde were generated as an oxygenated product of solvent toluene.

^{1}H NMR (400 MHz, $CDCl_3$, 303 K) for 4-*tert*-butylbenzaldehyde (**2b**)
δ 1.35 (s, 9H, ^{t}Bu), 7.81 (d, 2H, Ar), 7.55 (d, 2H, Ar), 9.98 (s, 1H, CHO).

^{1}H NMR (400 MHz, $CDCl_3$, 303 K) for 4-methoxybenzaldehyde (**2c**)
δ 3.89 (s, 3H, OMe), 7.84 (d, 2H, Ar), 9.89 (s, 1H, CHO).
Other signals of aromatic ring are overlapped with toluene.

^{1}H NMR (400 MHz, $CDCl_3$, 303 K) for 4-aminobenzaldehyde (**2d**)
δ 6.70 (d, 2H, Ar), 7.68 (d, 2H, Ar), 9.75 (s, 1H, CHO).

^{1}H NMR (400 MHz, $CDCl_3$, 303 K) for 4-hydroxybenzaldehyde (**2e**)
δ 7.00 (d, 2H, Ar), 7.75 (d, 2H, Ar), 9.83 (s, 1H, CHO).

^{1}H NMR (400 MHz, $CDCl_3$, 303 K) for 4-trifluoromethylbenzaldehyde (**2f**)
δ 7.80 (d, 2H, Ar), 8.00 (d, 2H, Ar), 10.09 (s, 1H, CHO).

^{1}H NMR (400 MHz, $CDCl_3$, 303 K) for 4-nitrobenzaldehyde (**2g**)
δ 8.08 (d, 2H, Ar), 8.40 (d, 2H, Ar), 10.16 (s, 1H, CHO).

^{1}H NMR (400 MHz, $CDCl_3$, 303 K) for 4-chlorobenzaldehyde (**2h**)
δ 7.49 (d, 2H, Ar), 7.80 (d, Ar), 9.96 (s, 1H, CHO).
Other signals of aromatic ring are overlapped with toluene.

^{1}H NMR (400 MHz, $CDCl_3$, 303 K) for 4-bromobenzaldehyde (**2i**)
δ 7.67 (d, Ar), 7.72 (d, Ar), 9.95 (s, 1H, CHO).
Other signals of aromatic ring are overlapped with toluene.

^{1}H NMR (400 MHz, $CDCl_3$, 303 K) for 4-iodobenzaldehyde (**2j**)
δ 7.58 (d, 2H, Ar), 7.91 (d, 2H, Ar), 9.95 (s, 1H, CHO).

^{1}H NMR (400 MHz, $CDCl_3$, 303 K) for 3-methoxylbenzaldehyde (**2k**)
δ 3.87 (s, 3H, OMe), 9.98 (s, 1H, CHO). Signals of aromatic ring are overlapped with toluene.

^{1}H NMR (400 MHz, $CDCl_3$, 303 K) for 3-trifluoromethylbenzaldehyde (**2l**)
δ 7.68 (t, 1H, Ar), 7.88 (d, 1H, Ar), 8.07 (d, 1H, Ar), 8.14 (s, 1H, Ar), 10.07 (s, 1H, CHO).

^{1}H NMR (400 MHz, $CDCl_3$, 303 K) for 3-fluorobenzaldehyde (**2m**)
δ 7.51 (m, Ar), 7.56 (m, Ar), 7.67 (m, Ar), 9.99 (s, 1H, CHO).
Other signals of aromatic ring are overlapped with toluene.

^{1}H NMR (400 MHz, $CDCl_3$, 303 K) for 3-chlorobenzaldehyde (**2n**)
δ 7.48 (m, Ar), 7.59 (m, Ar), 7.56 (m, 1H, Ar), 7.85 (m, 1H, Ar), 9.96 (s, 1H, CHO).
Other signals of aromatic ring are overlapped with toluene.

^{1}H NMR (400 MHz, $CDCl_3$, 303 K) for 2-methoxylbenzaldehyde (**2o**)
δ 3.93 (s, 3H, OCH_3), 7.84 (m, 2H, Ar), 10.41 (s, 1H, CHO).
Other signals of aromatic ring are overlapped with toluene.

^{1}H NMR (400 MHz, $CDCl_3$, 303 K) for 2-trifluoromethylbenzaldehyde (**2p**)
δ7.71 (m, Ar), 7.78 (m, Ar), 8.12 (m, 1H, Ar), 10.48 (s, 1H, CHO).
Other signals of aromatic ring are overlapped with toluene.

^{1}H NMR (400 MHz, $CDCl_3$, 303 K) for 2-fluorobenzaldehyde (**2q**)
δ 7.88 (m, 1H, Ar), 10.38 (s, 1H, CHO).
Other signals of aromatic ring are overlapped with toluene.

^{1}H NMR (400 MHz, $CDCl_3$, 303 K) for 2-bromobenzaldehyde (**2r**)
δ 7.64 (m, Ar), 7.91 (m, Ar), 10.37 (s, 1H, CHO).
Other signals of aromatic ring are overlapped with toluene.

^{1}H NMR (400 MHz, $CDCl_3$, 303 K) for heptadecanal (**2s**)
δ 9.76 (m, 1H, CHO). Signals of alkyl moiety are overlapped with starting carboxylic acid and toluene.

^{1}H NMR (400 MHz, $CDCl_3$, 303 K) for 8-nonenal (**2t**)
δ 5.01 (m, 2H, CH=CH_2), 5.82 (m, 1H, CH=CH_2), 9.77 (m, 1H, CHO).
Signals of alkyl moiety are overlapped with ^{t}BuOH, H_2O and toluene.

^{1}H NMR (400 MHz, $CDCl_3$, 303 K) for 5-heptenal (**2u**)
δ 5.01 (m, 2H, CH=CH_2), 5.82 (m, 1H, CH=CH_2), 9.75 (m, 1H, CHO).
Signals of alkyl moiety are overlapped with ^{t}BuOH, H_2O and toluene.

^{1}H NMR (400 MHz, $CDCl_3$, 303 K) for 8-heptadecenal (**2v**)
δ 5.35 (br, 2H, CH=CH), 9.75 (m, 1H, CHO).
Signals of alkyl moiety are overlapped with ^{t}BuOH, H_2O and toluene.

^{1}H NMR (400 MHz, $CDCl_3$, 303 K) for acetophenone (**2w**)

δ 7.94 (m, 2H, Ar), 2.60 (s, 3H, CH_3). Other signals of aromatic ring are overlapped with toluene.

^{1}H NMR (400 MHz, $CDCl_3$, 303 K) for diphenylketone (**2x**)

δ 7.80 (m, 2H, Ar). Other signals of aromatic ring are overlapped with toluene.

^{1}H NMR (400 MHz, $CDCl_3$, 303 K) for *N*-*tert*-butoxycarbonyl-1-pyrrolidin-2-one (**2y**)

δ 1.53 (s, 9H, ^{t}Bu), 1.99 (m, 2H), 3.73 (m, 2H). Other signals are overlapped with toluene.

^{1}H NMR (400 MHz, $CDCl_3$, 303 K) for 4-*tert*-butylbenzyl alcohol (**3b**)

δ1.32 (br, 9H, ^{t}Bu), 4.65 (br, 2H, CH_2). Signals of aromatic ring are overlapped with toluene.

^{1}H NMR (400 MHz, $CDCl_3$, 303 K) for 4-methoxybenzyl alcohol (**3c**)

δ 3.80 (s, 3H, CH_3), 4.62 (br, 2H, CH_2). Signals of aromatic ring are overlapped with toluene.

^{1}H NMR (400 MHz, $CDCl_3$, 303 K) for 4-hydroxybenzyl alcohol (**3e**)

δ 4.90 (br, 2H, CH_2), 6.87 (d, 2H, Ar), 7.23 (d, 2H, Ar).

^{1}H NMR (400 MHz, $CDCl_3$, 303 K) for 4-trifluoromethylbenzyl alcohol (**3f**)

δ 4.77 (br, 2H, CH_2). Signals of aromatic ring are overlapped with toluene.

^{1}H NMR (400 MHz, $CDCl_3$, 303 K) for 4-nitrobenzyl alcohol (**3g**)

δ 4.83 (br, 2H, CH_2), 7.53 (m, 2H, Ar), 8.22 (m, 2H, Ar).

^{1}H NMR (400 MHz, $CDCl_3$, 303 K) for 4-chlorobenzyl alcohol (**3h**)

δ 4.65 (d, 2H, CH_2). Signals of aromatic ring are overlapped with toluene.

^{1}H NMR (400 MHz, $CDCl_3$, 303 K) for 4-bromobenzyl alcohol (**3i**)

δ 4.62 (d, 2H, CH_2). Signals of aromatic ring are overlapped with toluene.

^{1}H NMR (400 MHz, $CDCl_3$, 303 K) for 4-iodobenzyl alcohol (**3j**)

δ 4.63 (d, 2H, CH_2). Signals of aromatic ring are overlapped with toluene.

^{1}H NMR (400 MHz, $CDCl_3$, 303 K) for 3-methoxybenzyl alcohol (**3k**)

δ 3.81 (s, 3H, OMe), 4.67 (br, 2H, CH_2). Signals of aromatic ring are overlapped with toluene.

^{1}H NMR (400 MHz, $CDCl_3$, 303 K) for 3-trifluoromethylbenzyl alcohol (**3l**)

δ 4.77 (br, 2H, CH_2). Signals of aromatic ring are overlapped with toluene.

^{1}H NMR (400 MHz, $CDCl_3$, 303 K) for 3-fluorobenzyl alcohol (**3m**)

δ 4.69 (d, 2H, CH_2). Signals of aromatic ring are overlapped with toluene.

^{1}H NMR (400 MHz, $CDCl_3$, 303 K) for 3-chlorobenzyl alcohol (**3n**)

δ 4.66 (d, 2H, CH_2). Signals of aromatic ring are overlapped with toluene.

^{1}H NMR (400 MHz, $CDCl_3$, 303 K) for 2-methoxylbenzyl alcohol (**3o**)

δ 3.87 (s, 3H, OCH_3). 4.76 (d, 2H CH_2). Signals of aromatic ring are overlapped with toluene.

^{1}H NMR (400 MHz, $CDCl_3$, 303 K) for 2-trifluoromethylbenzyl alcohol (**3p**)

δ 4.88 (d, 2H, CH_2). Signals of aromatic ring are overlapped with toluene.

^{1}H NMR (400 MHz, $CDCl_3$, 303 K) for 2-fluorobenzyl alcohol (**3q**)

δ 4.76 (d, 2H, CH_2). Signals of aromatic ring are overlapped with toluene.

^{1}H NMR (400 MHz, $CDCl_3$, 303 K) for 2-bromobenzyl alcohol (**3r**)

δ 4.69 (d, 2H, CH_2). Signals of aromatic ring are overlapped with toluene.

^{1}H NMR (400 MHz, $CDCl_3$, 303 K) for 1-heptadecanol (**3s**)

δ 3.62 (m, 2H). Signals of alkyl moiety are overlapped with ^{t}BuOH, H_2O and toluene.

^{1}H NMR (400 MHz, $CDCl_3$, 303 K) for 8-nonen-1-ol (**3t**)

δ 3.64 (br, 2H, C*H*$_2$OH), 5.01 (m, 2H, CH=C*H*$_2$), 5.82 (m, 1H, C*H*=CH_2).

Signals of alkyl moiety are overlapped with ^{t}BuOH, H_2O and toluene.

^{1}H NMR (400 MHz, $CDCl_3$, 303 K) for 5-hepten-1-ol (**3u**)

δ 3.64 (br, 2H, C*H*$_2$OH), 5.01 (m, 2H, CH=C*H*$_2$), 5.82 (m, 1H, C*H*=CH_2).

Signals of alkyl moiety are overlapped with ^{t}BuOH, H_2O and toluene.

^{1}H NMR (400 MHz, $CDCl_3$, 303 K) for 8-heptadecen-1-ol (**3v**)

δ 3.63 (m, 2H, C*H*$_2$OH), 5.35 (br, 2H, CH=CH).

Signals of alkyl moiety are overlapped with ^{t}BuOH, H_2O and toluene.

^{1}H NMR (400 MHz, $CDCl_3$, 303 K) for 1-phenylethanol (**3w**)

δ 4.91 (s, 1H, CH). Other signals of aromatic ring and a methyl group are overlapped toluene and H_2O.

^{1}H NMR (400 MHz, $CDCl_3$, 303 K) for diphenylmethanol (**3x**)

δ 5.83 (s, 1H, CH). Other signals of aromatic ring are overlapped with toluene.

^{1}H NMR (400 MHz, $CDCl_3$, 303 K) for peroxy lactone **10**

δ 1.68 (s, 6H, CH_3), 7.64 (m, 1H, Ar), 8.14 (m, 1H, Ar).

Other signals of aromatic ring are overlapped with toluene.

^{1}H NMR (400 MHz, $CDCl_3$, 303 K) for 3,3-dimethylphthalide (**11**)

δ 1.66 (s, 6H, CH_3), 7.64 (m, 1H, Ar), 7.87 (m, 1H, Ar).

Other signals of aromatic ring are overlapped with toluene.

^{1}H NMR (400 MHz, $CDCl_3$, 303 K) for biphenyl-2,2'-carbolactone (**13**)

δ 7.59 (m, 1H, Ar), 7.83 (m, 1H, Ar), 8.08 (m, 1H, Ar), 8.14 (m, 1H, Ar), 8.42 (m, 1H, Ar).

Other signals of aromatic ring are overlapped with toluene.

XIX. ^{1}H NMR Spectra of Catalytic Reaction Mixtures

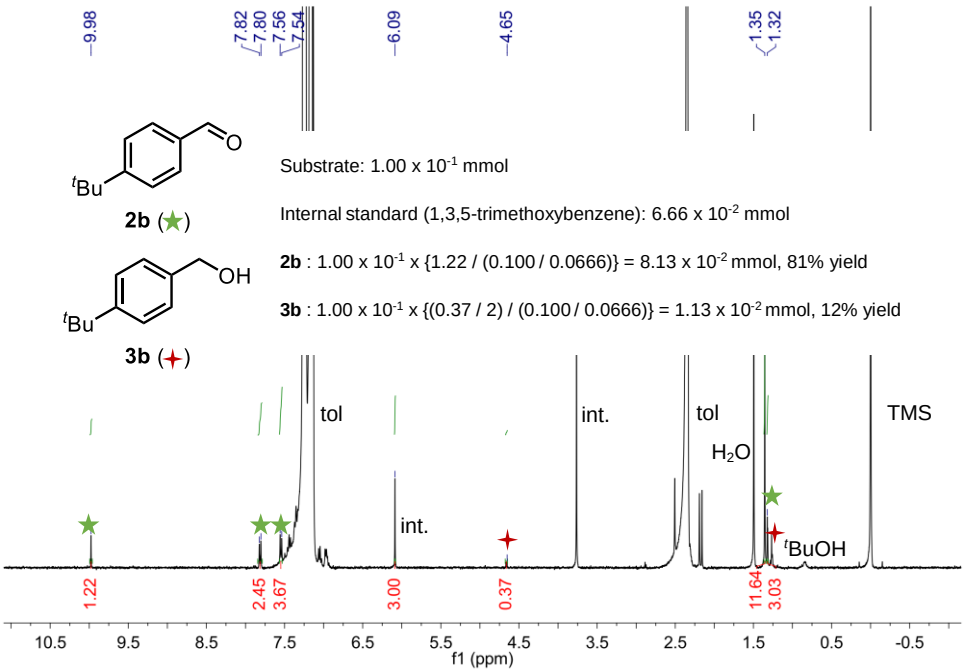

Figure S24. ^{1}H NMR spectrum of the reaction mixture of **2b** and **3b**.

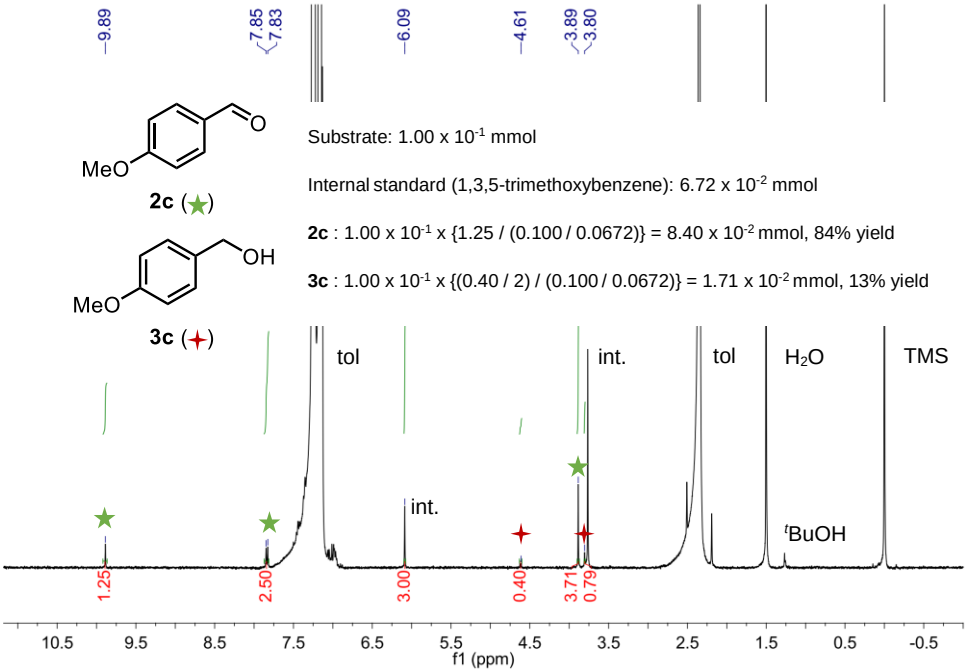

Figure S25. ^{1}H NMR spectrum of the reaction mixture of **2c** and **3c**.

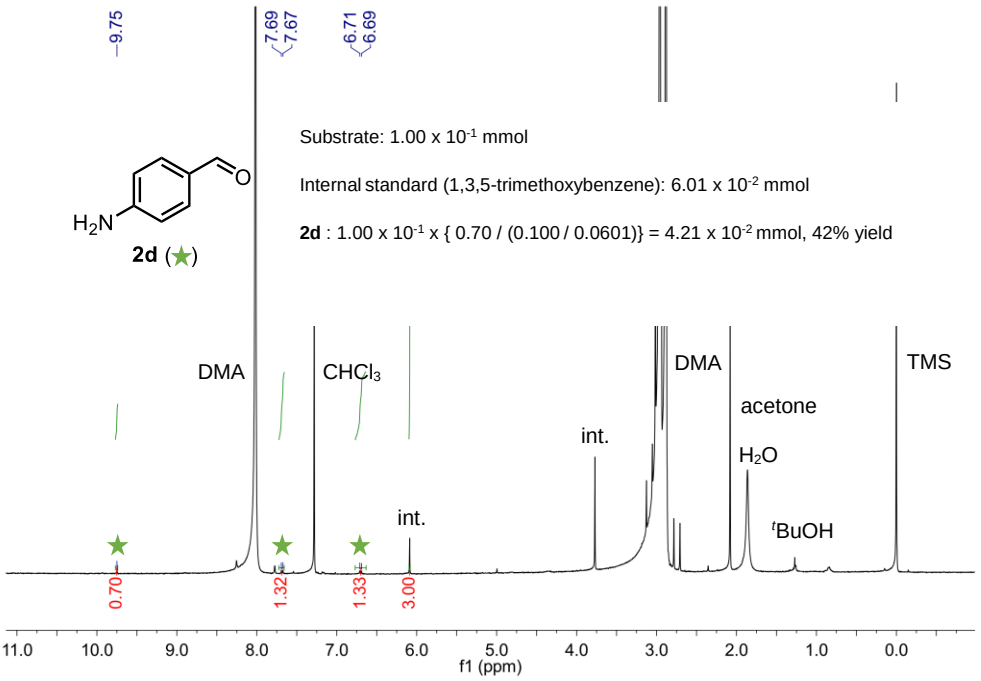

Figure S26. ^{1}H NMR spectrum of the reaction mixture of **2d**.

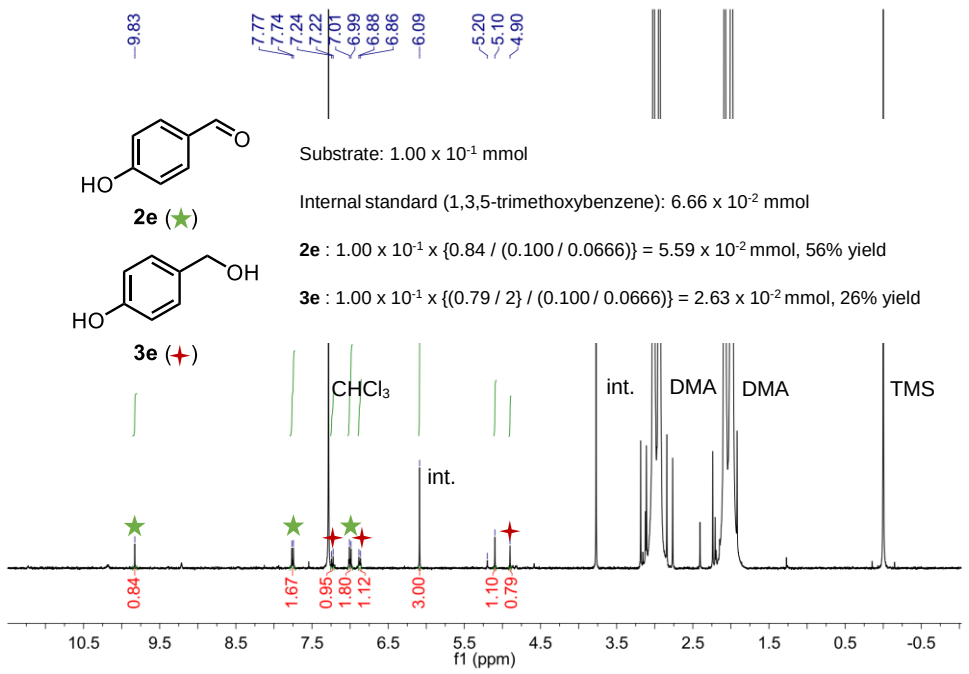

Figure S27. ^{1}H NMR spectrum of the reaction mixture of **2e** and **3e**.

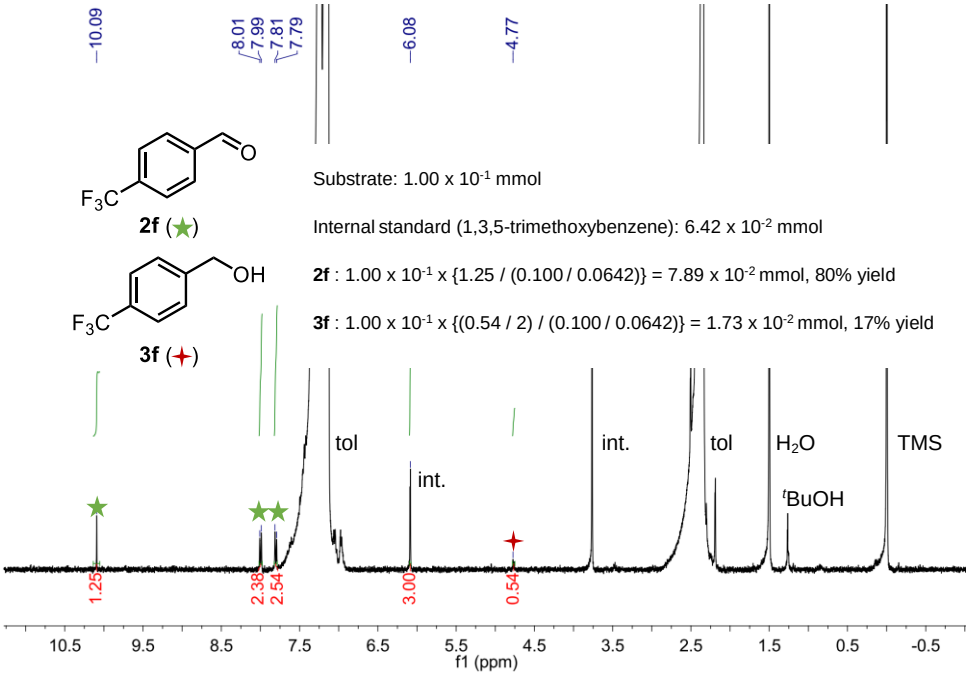

Figure S28. ^{1}H NMR spectrum of the reaction mixture of **2f** and **3f**.

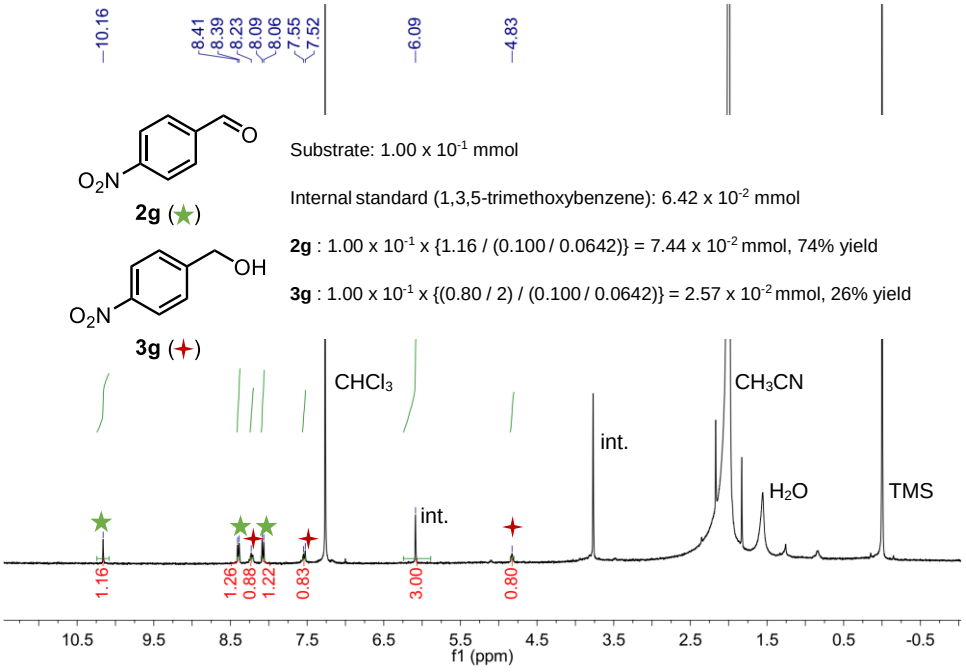

Figure S29. ^{1}H NMR spectrum of the reaction mixture of **2g** and **3g**.

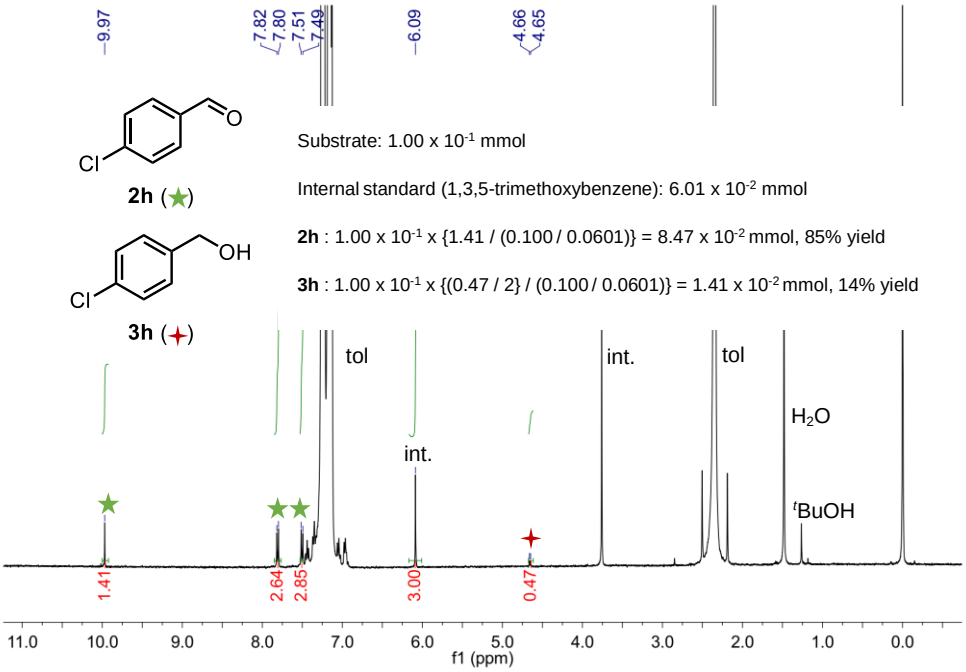

Figure S30. ^{1}H NMR spectrum of the reaction mixture of **2h** and **3h**.

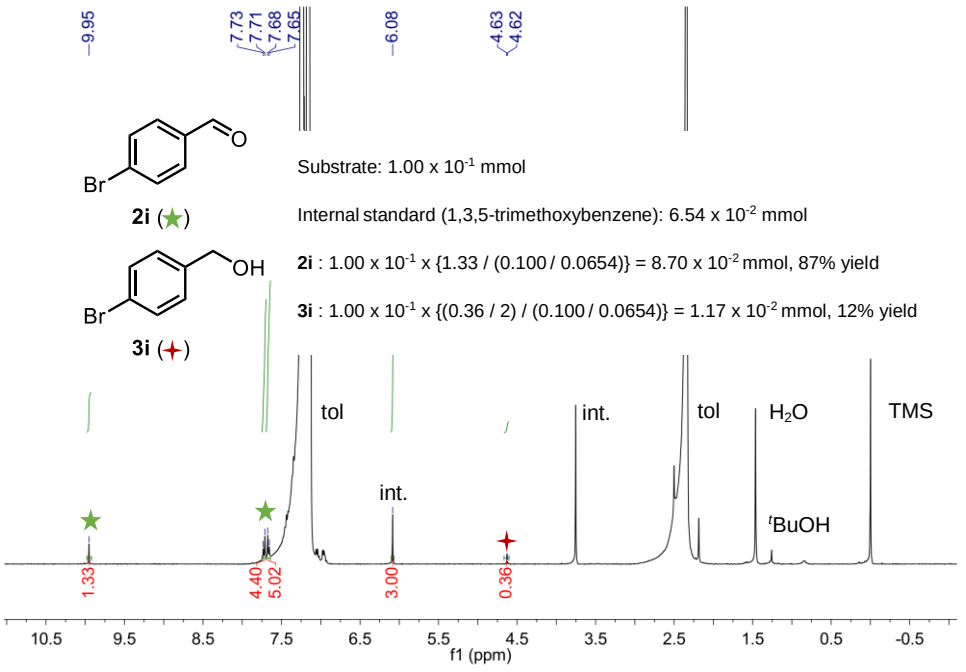

Figure S31. ^{1}H NMR spectrum of the reaction mixture of **2i** and **3i**.

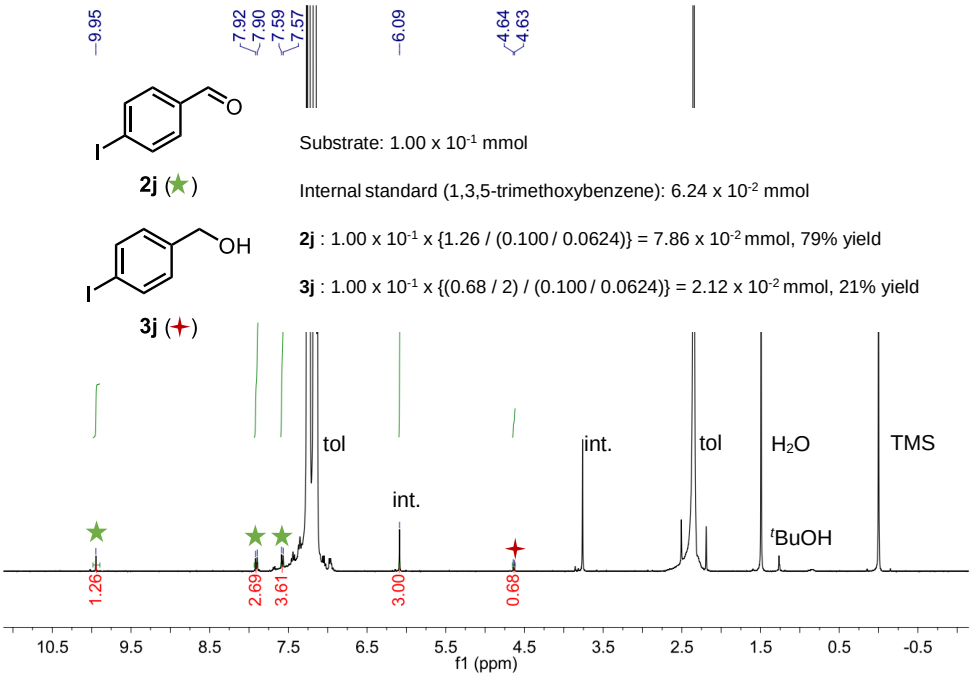

Figure S32. ^{1}H NMR spectrum of the reaction mixture of **2j** and **3j**.

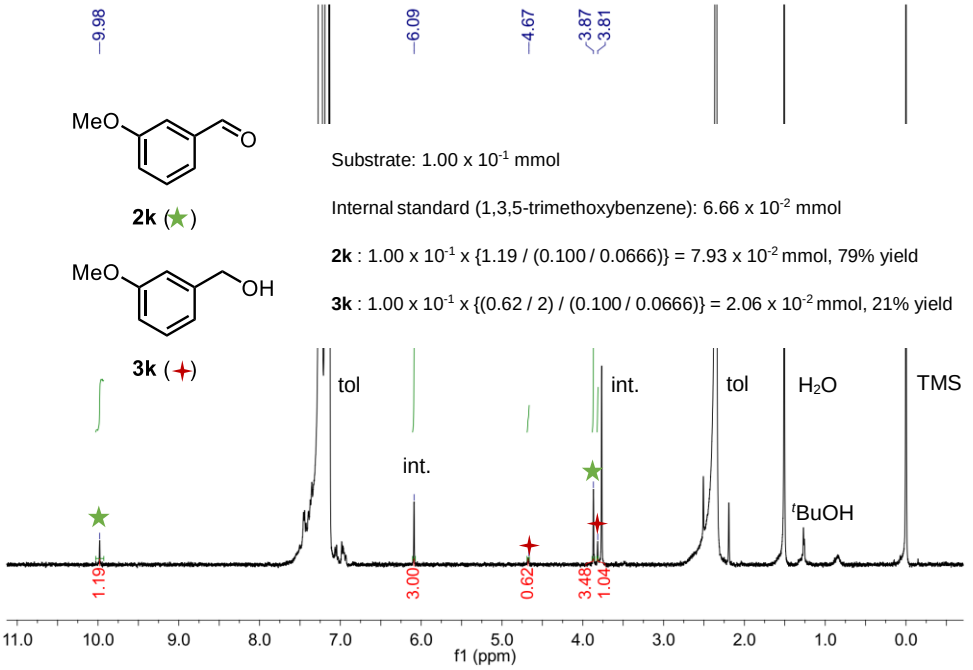

Figure S33. ^{1}H NMR spectrum of the reaction mixture of **2k** and **3k**.

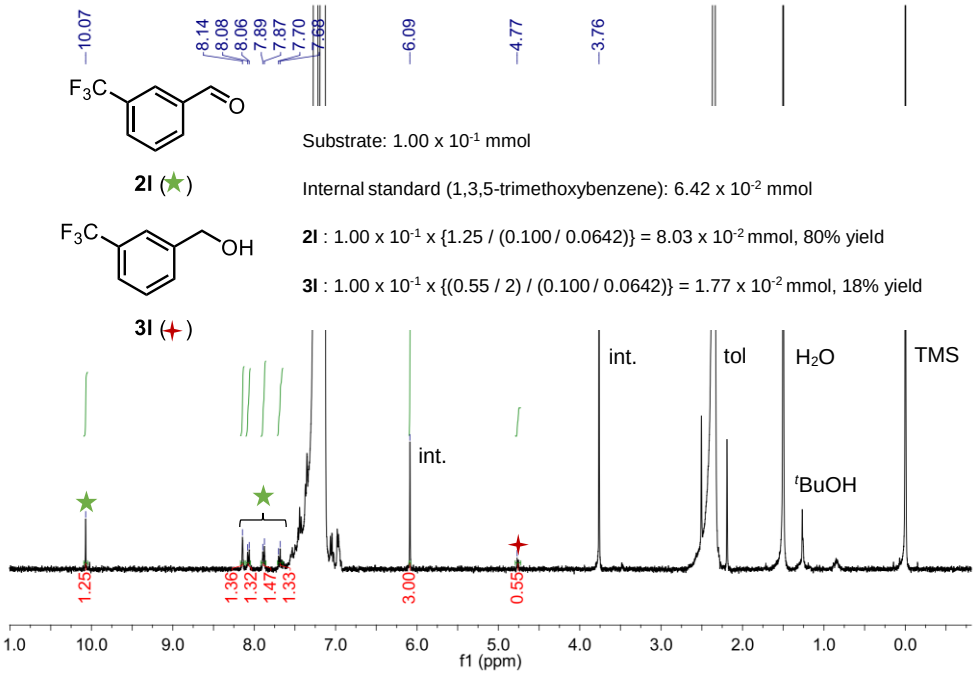

Figure S34. ^{1}H NMR spectrum of the reaction mixture of **2l** and **3l**.

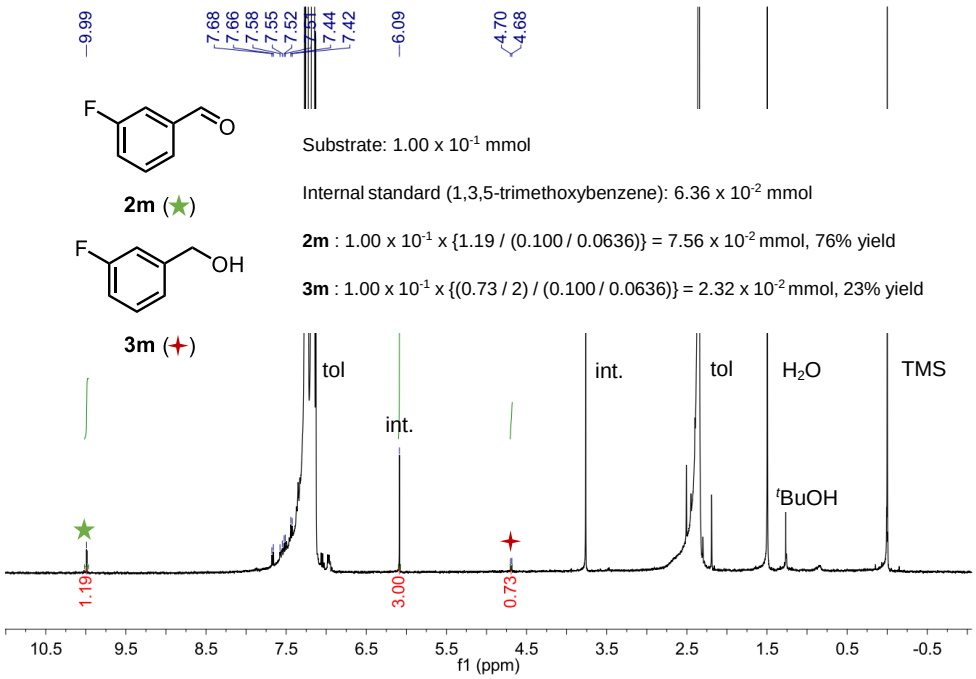

Figure S35. ^{1}H NMR spectrum of the reaction mixture of **2m** and **3m**.

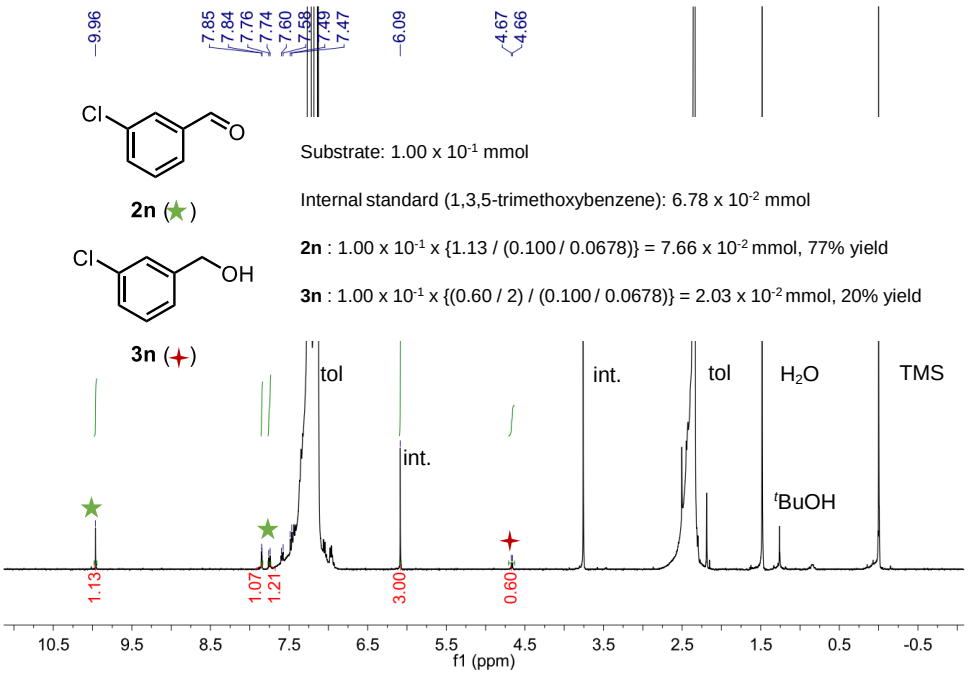

Figure S36. ^{1}H NMR spectrum of the reaction mixture of **2n** and **3n**.

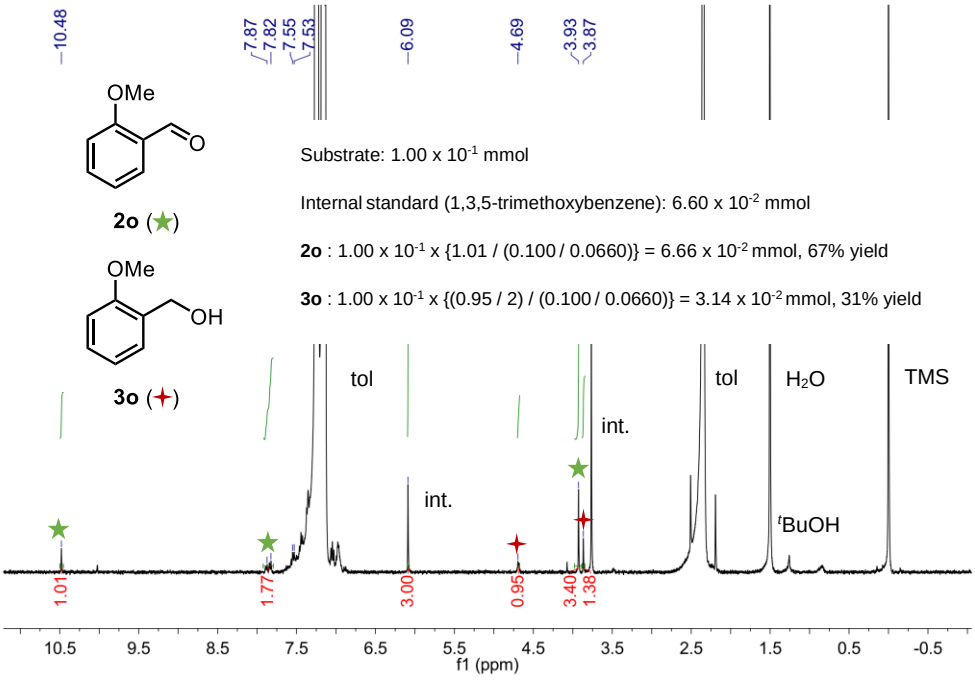

Figure S37. ^{1}H NMR spectrum of the reaction mixture of **2o** and **3o**.

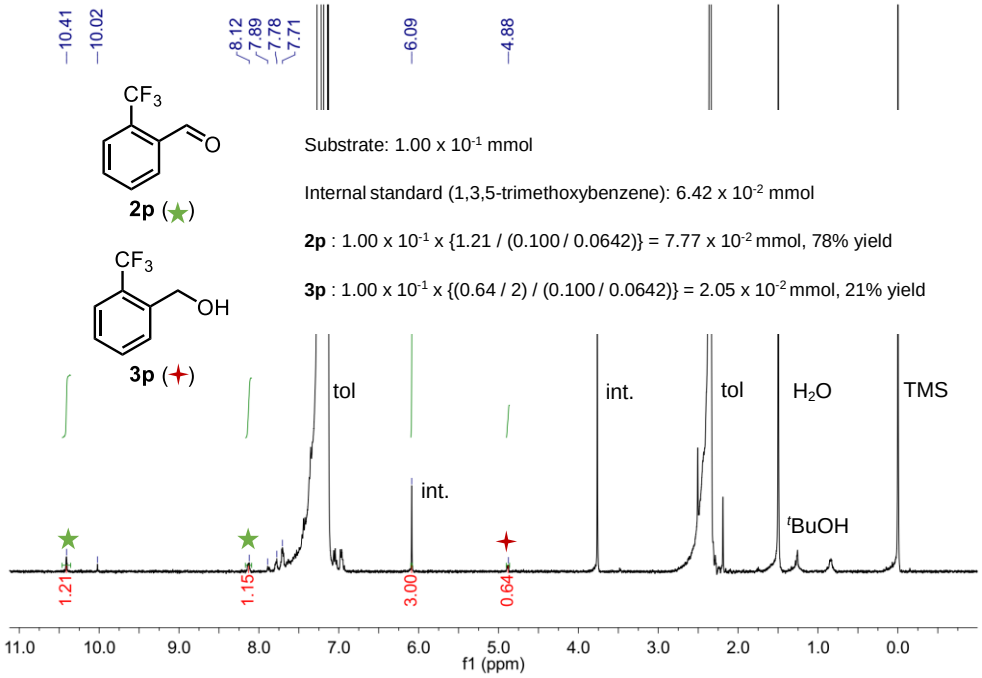

Figure S38. [1]H NMR spectrum of the reaction mixture of **2p** and **3p**.

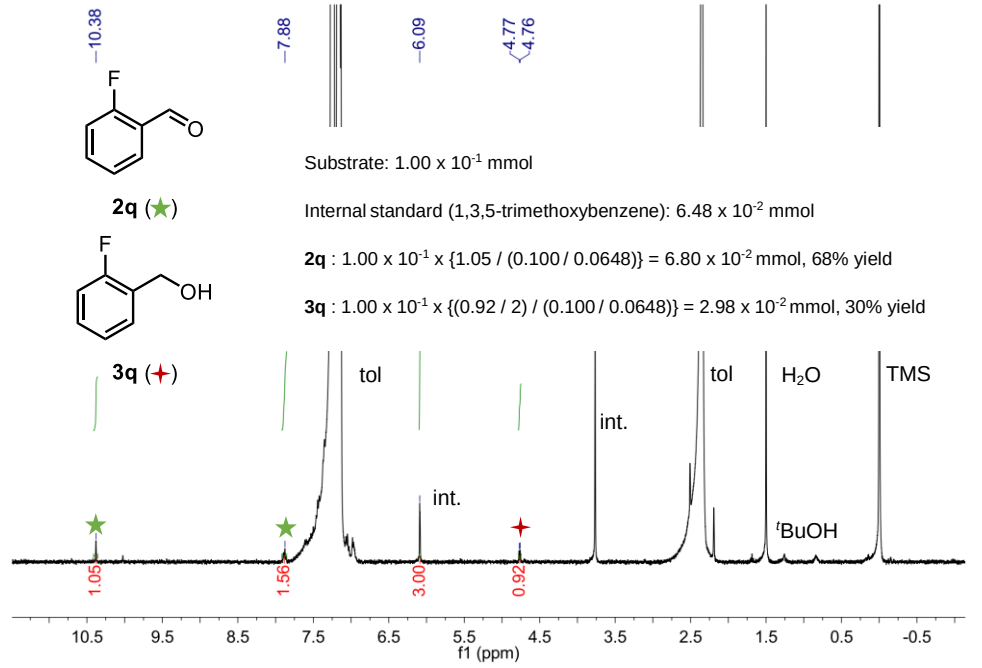

Figure S39. [1]H NMR spectrum of the reaction mixture of **2q** and **3q**.

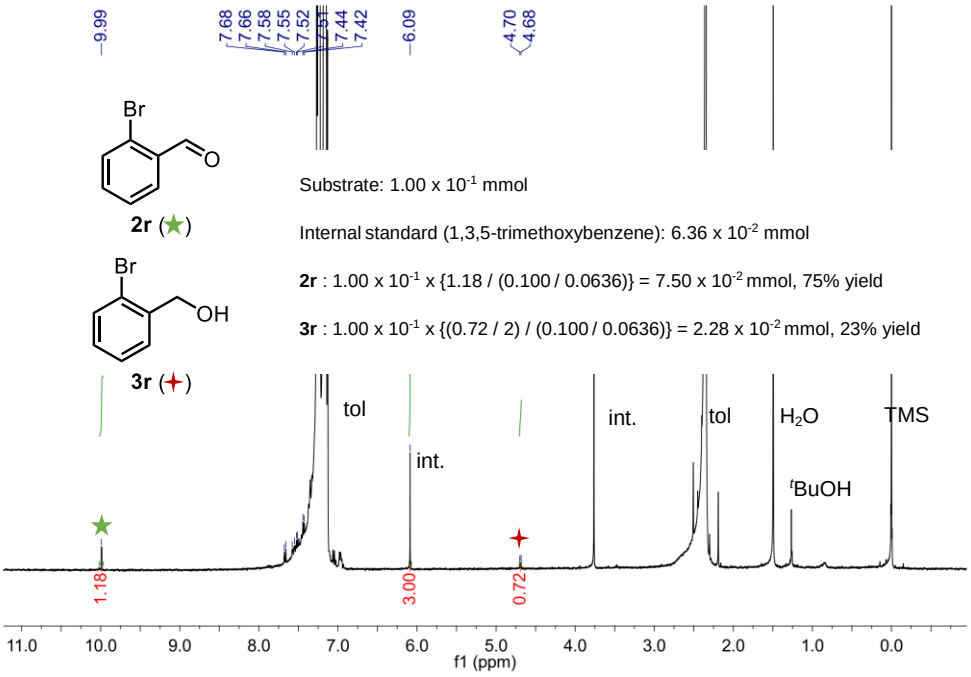

Figure S40. ^{1}H NMR spectrum of the reaction mixture of **2r** and **3r**.

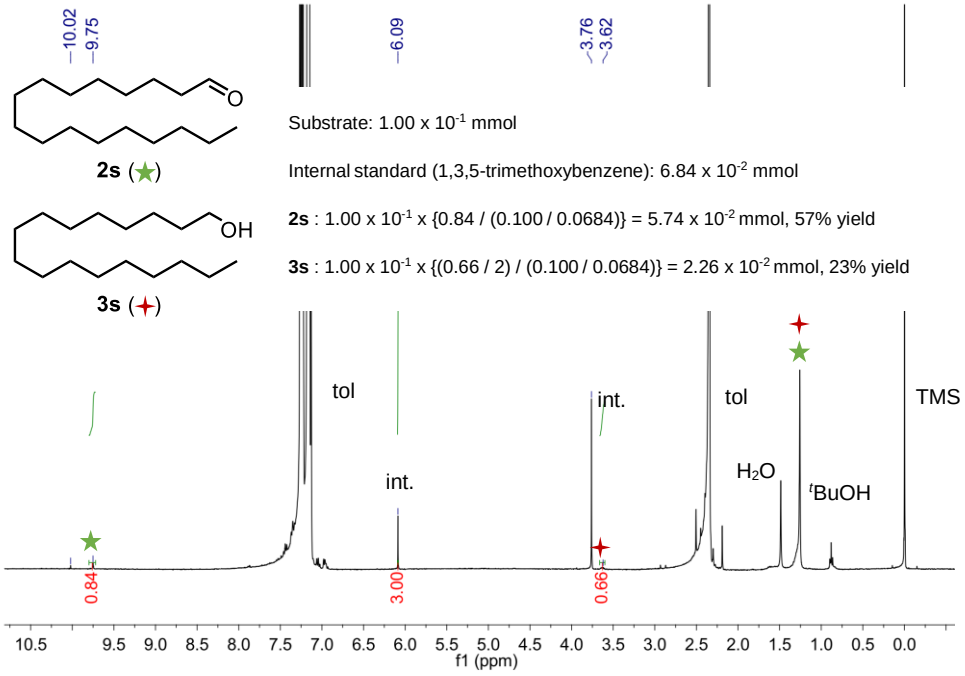

Figure S41. ^{1}H NMR spectrum of the reaction mixture of **2s** and **3s**.

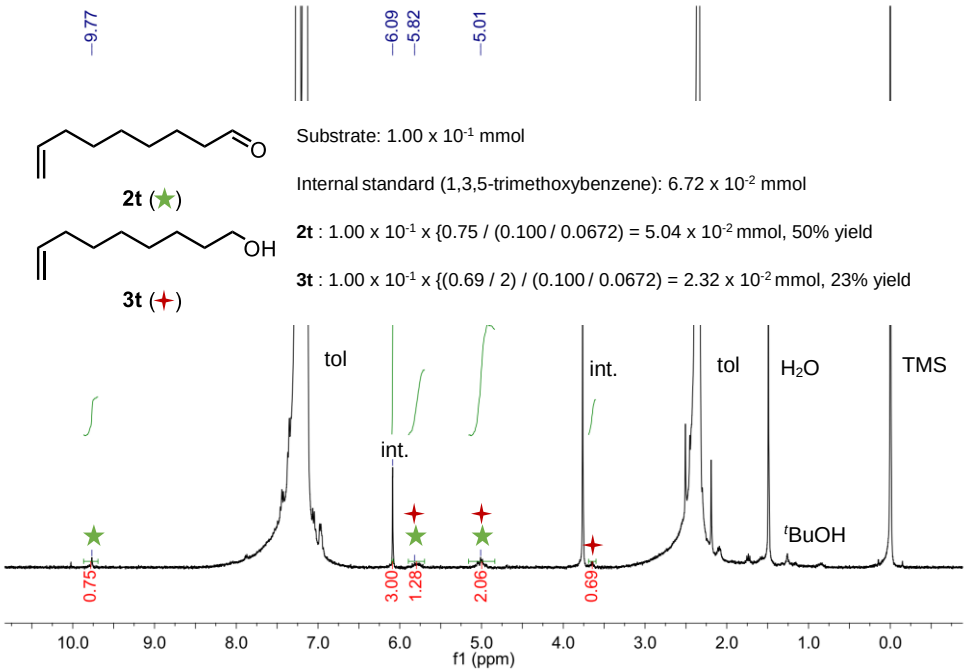

Figure S42. ^{1}H NMR spectrum of the reaction mixture of **2t** and **3t**.

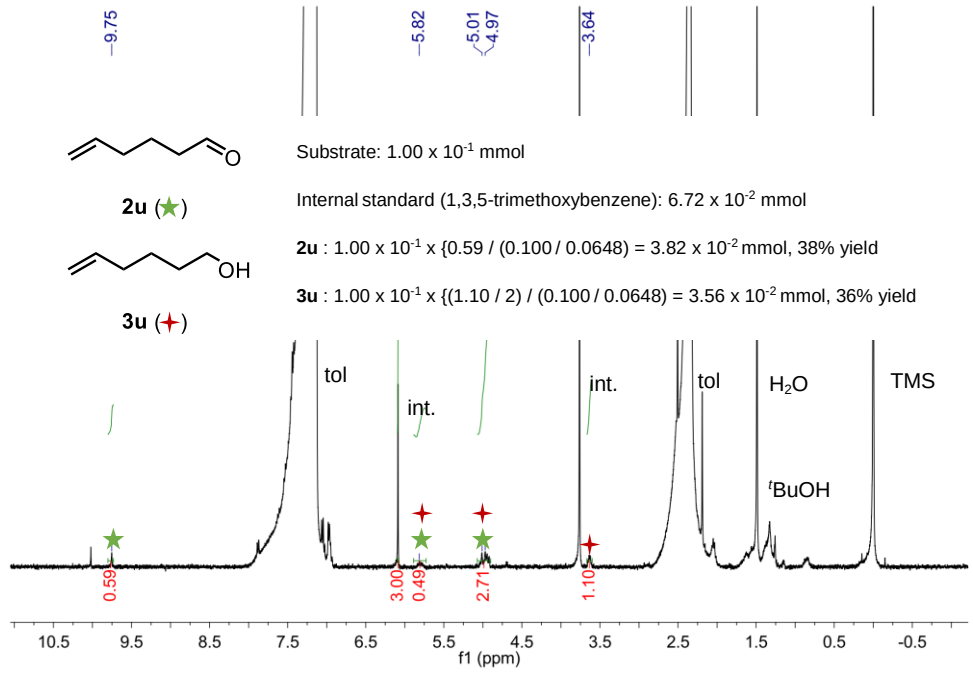

Figure S43. ^{1}H NMR spectrum of the reaction mixture of **2u** and **3u**.

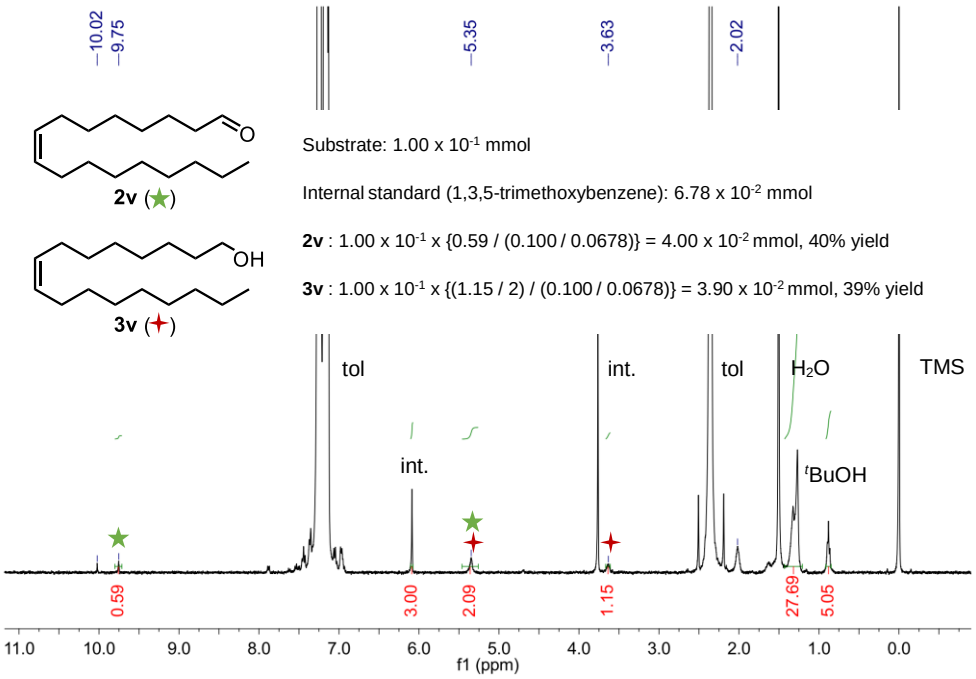

Figure S44. ^{1}H NMR spectrum of the reaction mixture of **2v** and **3v**.

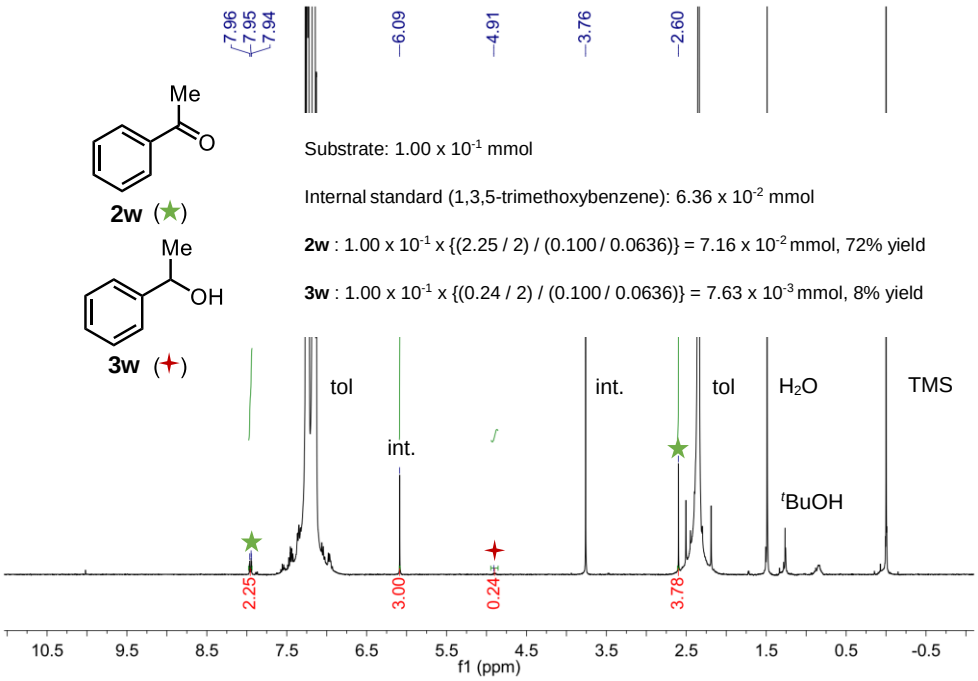

Figure S45. ^{1}H NMR spectrum of the reaction mixture of **2w** and **3w**.

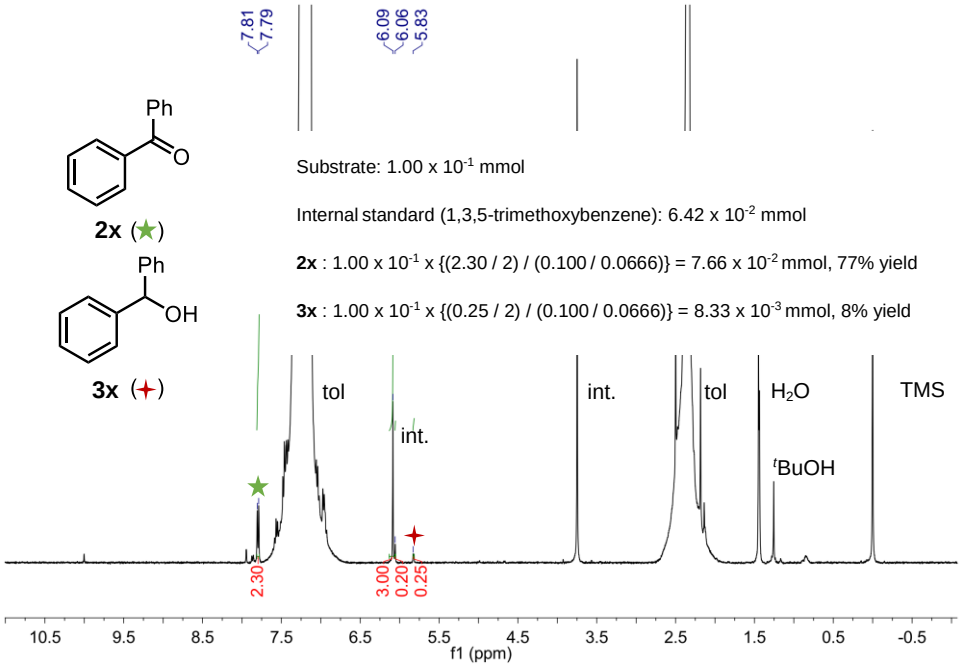

Figure S46. ^{1}H NMR spectrum of the reaction mixture of **2x** and **3x**.

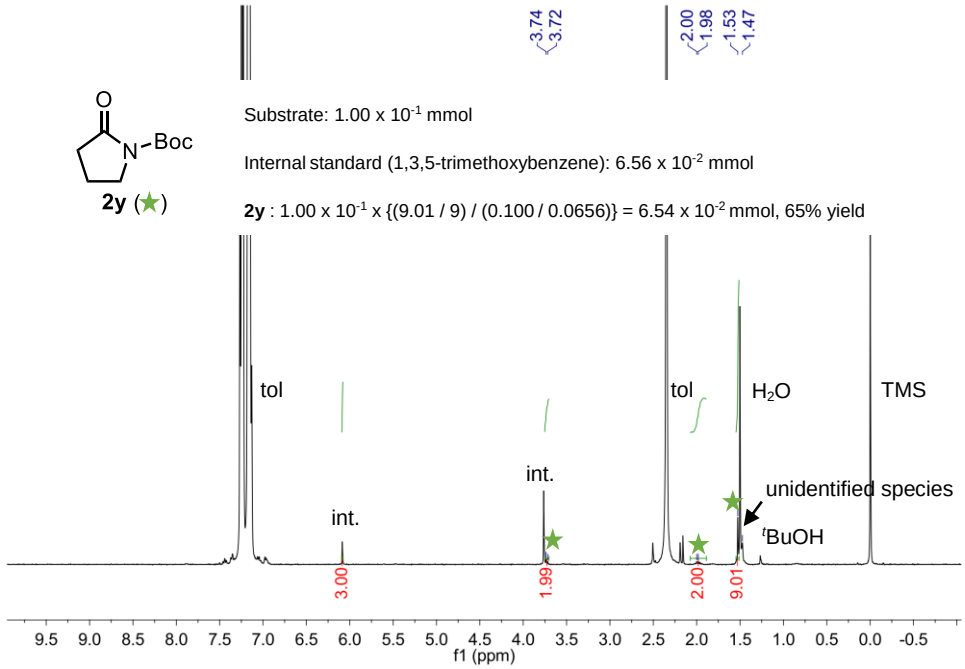

Figure S47. ^{1}H NMR spectrum of the reaction mixture of **2y**.

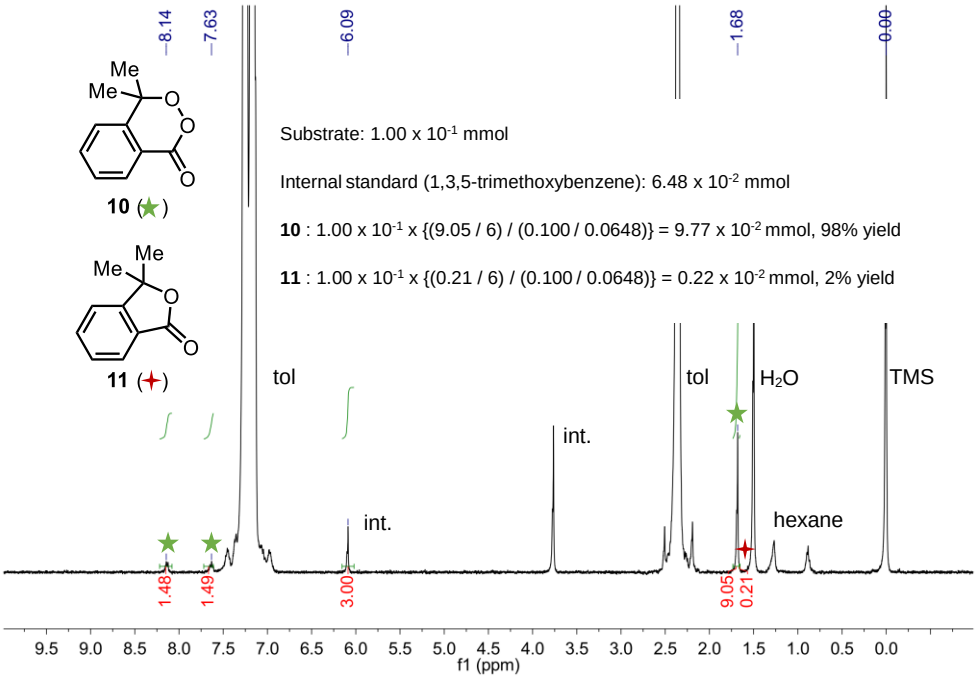

Figure S48. ^{1}H NMR spectrum of the reaction mixture of **10** and **11** (1 mol% of Ce(O^{t}Bu)$_4$ under 1 atm of O_2) (Table 4, entry 1).

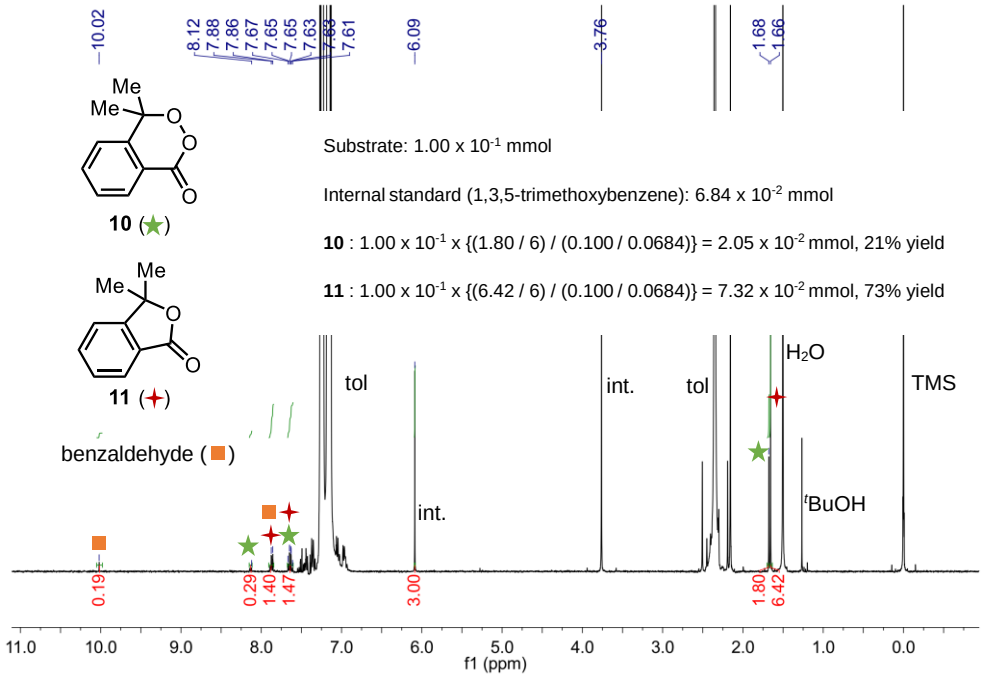

Figure S49. ^{1}H NMR spectrum of the reaction mixture of **10** and **11** (20 mol% of catalyst, under air) (Table 4, entry 4).

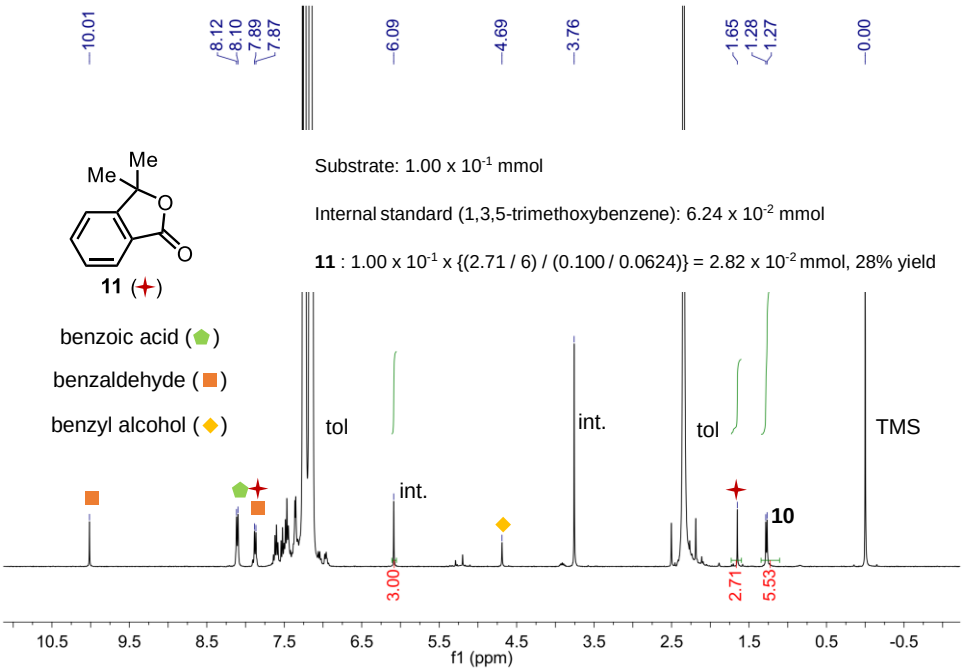

Figure S50. ^{1}H NMR spectrum of the reaction mixture of **10** and **11** (5 mol% of $Fe(OAc)_2$, under air) (Table 4, entry 6).

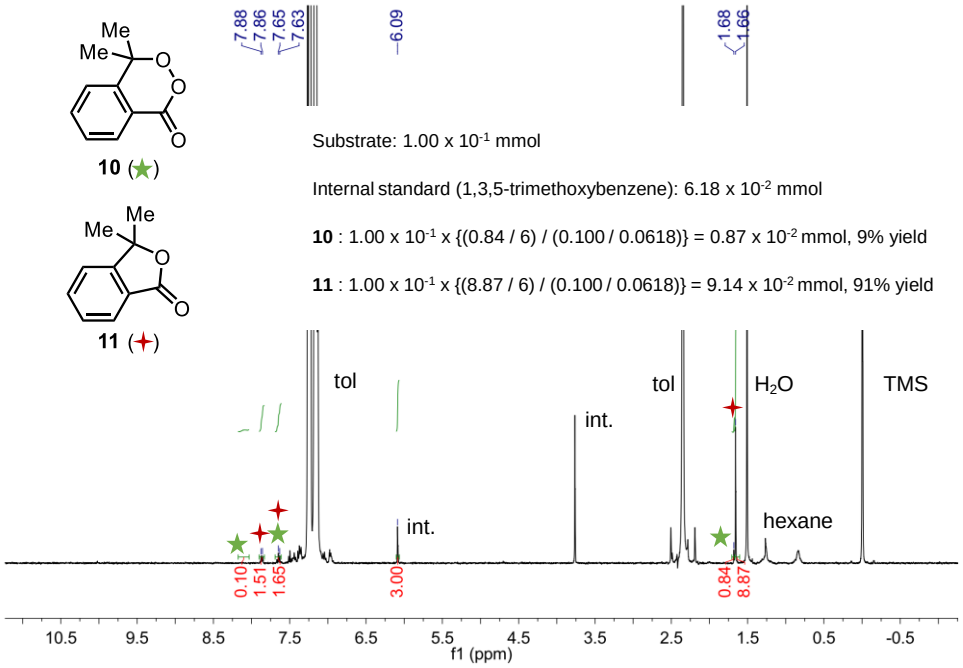

Figure S51. ^{1}H NMR spectrum of the reaction mixture of **10** and **11** (5 mol% of $Ce(O^tBu)_4$, 5 mol% of $Co(acac)_2{\cdot}2H_2O$, under air, in a 5 mL Schlenk) (Table 4, entry 7).

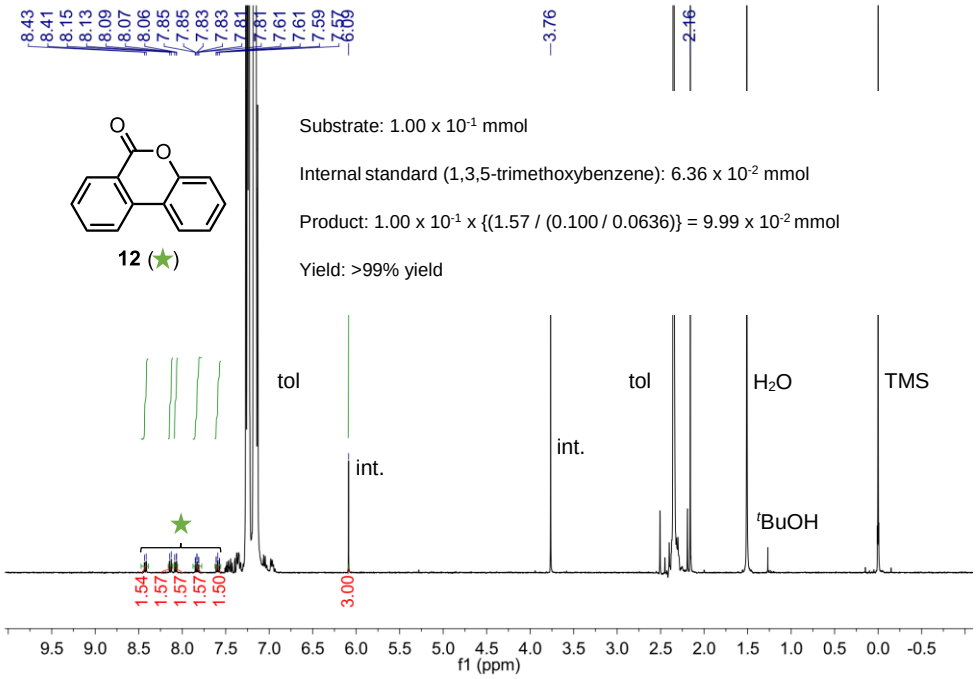

Figure S52. ^{1}H NMR spectrum of the reaction mixture of **12**.

XX. Crystal Data and Data Collection Parameters of 6[a]

complex	**6**
empirical fomula	$C_{96}H_{180}Ce_6O_{40}$
formula weight	2815.17
cryst. system	Triclinic
space group	$P\bar{1}$ (#2)
a, Å	15.2401(4)
b, Å	15.6758(2)
c, Å	15.7321(4)
a, deg	64.493(3)
b, deg	76.630(4)
g, deg	65.590(4)
V, Å^3	3082.38(17)
Z	1
Dcald, g/cm^3	1.516
μ [Mo-*K*α], cm^{-1}	22.417
T, K	113
crystal size	0.220 x 0.200 x 0.200
θ range for data collection (deg)	3.073, 25.242
no. of reflections measured	71088
Unique data (*R*int)	0.0301
data / restraints / parameters	14122/0/685
*R*1 ($I > 2.0\sigma(I)$)	0.0365
*wR*2 ($I > 2.0\sigma(I)$)	0.1033
R1 (all data)	0.0399
*wR*2 (all data)	0.1016
GOF on F^2	1.096
Δρ, e Å^{-3}	3.44, -1.53

(a) $R1 = (\Sigma||Fo| - |Fc||)/(\Sigma|Fo|)$, $wR2 = [\{\Sigma w(Fo^2 - Fc^2)^2\}/\{\Sigma w(Fo^4)\}]^{1/2}$

References

[1] Pangborn, A. B.; Giardello, M. A.; Grubbs, R. H.; Rosen, R. K.; Timmers, F. J. Safe and Convenient Procedure for Solvent Purification. *Organometallics* **1996**, *15*, 1518-1520.

[2] Arnold, P. L.; Casely, I. J.; Zlatogorsky, S.; Wilson, C. Organometallic cerium complexes from tetravalent coordination complexes. *Helv. Chim. Acta* **2009**, *92*, 2291-2303.

[3] Reich, H. J. WinDNMR: Dynamic NMR Spectra for Windows. *J. Chem. Educ.*, **1995**, *72*, 1086.

[4] Hermans, I.; Peeters, J.; Vereecken, L.; Jacobs, P. A. Mechanism of Thermal Toluene Autoxidation. *ChemPhysChem* **2007**, *8*, 2678–2688.